Proc Indian Natn Sci Acad, **70, A,** No. 4, July 2004, pp. 555–577

POTENTIAL OF *IN VIVO* MAGNETIC RESONANCE SPECTROSCOPY (MRS) IN MEDICINE

UMA SHARMA AND N R JAGANNATHAN*

Department of NMR, All India Institute of Medical Sciences, New Delhi-110029 (India)

(Received 07 January 2003 ; Accepted 10 February 2003)

The technique of NMR has developed over the years as the principal method for determining the molecular structure and conformation of biomolecules. It has a major impact in the last two decades in understanding and managing various disease processes that affect humans through magnetic resonance imaging (MRI). MRI is noninvasive and provides anatomic images in multiple planes enabling tissue characterization. *In vivo* magnetic resonance spectroscopy (MRS), on the other hand, is useful technique for assessing the biochemical status of normal and pathological tissue. Among the various nuclei that generate MR signal, proton (^{1}H), phosphorus (^{31}P) and carbon (^{13}C) are most important in the study of the biochemistry of living systems. Nuclei such as fluorine (^{19}F) and lithium (^{7}Li) are used to study the pharmacokinetics of drugs while sodium (^{23}Na) and potassium (^{39}K) MRS provides information on several physiological, biochemical and transport processes. Being noninvasive, MRS can also be used repetitively for assessment of the response of the tumor to various therapeutic regimens and for evaluating the efficacy of drugs at the molecular level. In the last two decades *in vivo* MRS has emerged as a unique tool in the diagnosis of various disease processes with metabolic information for studying the tissue metabolism. This review presents an overview of the various aspects of localized *in vivo* MRS methodologies with examples on the clinical applications of ^{1}H and ^{31}P MRS in brain, breast and muscle.

Key Words : ***In vivo*** **^{1}H and ^{31}P Magnetic Resonance Spectroscopy (MRS); Image Guided; Localization Techniques; Single Voxel; Chemical Shift Imaging; Tumor; Response to Therapy**

1 Introduction

Since the first experiments of nuclear magnetic resonance (NMR) in 1946, the application of this technique in different areas like physics, chemistry, biology and medicine has been phenomenal. The most familiar application of NMR phenomenon to the common man and the clinical community is magnetic resonance imaging (MRI), which is used to produce anatomic images for diagnostic purposes for various pathologies[1-3]. Lauterbur[4] in 1973 produced the first image of a live animal. Later with the development of long-hold magnets with high homogeneity, strong magnetic field gradients, RF electronics, and powerful computers, the whole body MRI systems became a reality for many clinical applications. MRI produces a spatial display of the distribution of nuclei (such as hydrogens) and provides a high-resolution morphological picture (anatomical information) with superior contrast resolution compared to other currently available imaging modalities. Moreover MRI is noninvasive, uses no ionizing radiations such as X-rays and images can be obtained in transverse, sagittal, coronal and oblique planes without moving the object/subject. Being noninvasive, the method can be used for repetitive measurements, which is useful to study the pharmacokinetics and efficacy of drugs. These features have made MRI as one of the most useful soft tissue diagnostic modality for many neurological, cardiac, musculoskeletal and other pathologies[1-3].

The other important application of NMR phenomenon in clinical medicine is NMR spectroscopic investigation of living systems termed as '*in vivo* MR spectroscopy' (MRS). MRI and *in vivo* MRS, both are based on the same physical phenomenon as NMR and the principles are described in many books[1-3,5-8]. The significant technical difference between MRI and MRS is that in MRI the signal is acquired in the presence of magnetic field gradients while for MRS it is prerequisite to have a homogeneous magnetic field to observe the chemical shift differences of metabolites and therefore no magnetic field gradients are applied during signal acquisition. MRI and *in vivo* MRS have evolved more or less independently, however, most *in vivo* localized MRS use MR images to guide the region of interest (ROI) or volume of interest (VOI) for spectroscopic investigations. Thus the success of MRI had considerable impact in the development of *in vivo*

*Author for Correspondence : *Fax :* 011-2658 8663;
E-mail: jagan1954@hotmail.com

MRS methodologies, which can be used to detect and estimate the concentration of different metabolites present in a particular region of the tissue or organ. The relative levels of these metabolites provide information on the status of normal and pathological tissues. The technique can also be used repetitively to monitor the response of tumors to various therapeutic modalities, efficacy of drugs and to understand the different metabolic processes[2,6-8]. In principle, *in vivo* MRS of organs and tissues in humans/animals are an extension of the high-resolution NMR used for identification of chemicals and their structure, but applied to more complex systems.

Nuclei that have high natural abundance and sensitivity in living systems are most suitable for *in vivo* MRS. For these reasons, most of the applications of *in vivo* MRS have been using ^{1}H and ^{31}P nuclei[1-8]. In living systems, there are two main sources of protons namely water and fat that are used for image formation in MRI. However, the protons of water and fat mask the signals of metabolites that are present in low concentration in tissues. Therefore, the detection of resonances of biochemicals with low concentration requires special techniques for suppression of water signal[9-12] (*vide infra*). The aim of *in vivo* MRS is to obtain a spectrum that arises exclusively from the VOI, with the best achievable sensitivity and with minimum contribution from other regions. While a multitude of localization schemes have been proposed; however, the techniques that are in clinical use today are limited. A comprehensive review of all the localization techniques published to date is beyond the scope of this article and many excellent books[2, 6,8,13] and reviews[14, 15] are available, the reader may refer to them. The approach taken in this review is to provide a brief overview of the observable metabolites in various organs using the various acquisition methodologies. MRS can be performed with a large number of isotopes; however, the focus of this review is on the application of ^{1}H and ^{31}P MRS in the study of muscle, brain and breast.

2 Localization Techniques in *in vivo* MR Spectroscopy

In vivo MRS began with the analysis of isolated tissues and surface regions from intact animals. Later, the availability of gradients for MRI led to the development of localization techniques that obtain spectra from single volumes of tissues. The basic requirement of *in vivo* localized MRS, as pointed out earlier, is to acquire the signal from a particular VOI with optimal sensitivity. Table-I presents a brief summary of some of the available localization techniques that are in clinical use today. Magnetic field gradients in either the $\mathbf{B}_0$ field as in imaging or in the $\mathbf{B}_1$ (RF) field are used for localization of a particular volume. One of the earliest methods for localization of VOI is to employ surface coils. In general, MRS requires a homogeneous $\mathbf{B}_0$ field for signal acquisition and imposition of a gradient in $\mathbf{B}_0$ for localization bring with it the problem of eddy currents. These are currents induced in the magnet conductive structures during the gradient switching that

Table I

Different Localization MR Techniques used in Clinical Research

No.	Localization Schemes	Method	Uses
1.	Surface Coil	Normally a circular coils positioned close to the anatomy of interest	To obtain spectra from surface and superficial tumors.
	(a) Rotating frame Zeugmatography	$\mathbf{B}_1$ gradient	Useful to get spectra the from various depth along the axis of surface coil
	(b) Topical magnetic resonance (TMR)	$\mathbf{B}_0$ inhomogeneoities	Detects signal from a large VOI
	(c) DRESS	$\mathbf{B}_0$ slice selection gradient	Can detect signal from slices parallel to the plane of surface coil
2.	ISIS	$\mathbf{B}_0$ slice selection gradient and inversion RF pulses	1D ISIS measures signal from a slice 2D ISIS measures signal from a small column 3D ISIS measures signal from a voxel
3.	STEAM	$\mathbf{B}_0$ slice selection gradient	Spectra can be obtained from tumors which are deep inside the organ. Single voxel localization technique
4.	PRESS	$\mathbf{B}_0$ slice selection gradient	Spectra can be obtained from tumors which are deep inside the organ. Single voxel localization technique
5.	CSI or SI	$\mathbf{B}_0$ phase encoding gradient and $\mathbf{B}_0$ slice selection gradient	Multi voxel technique 1D, 2D and 3D acquisition is possible

result in transient inhomogeneities in $\mathbf{B}_0$. The early localization methods like rotating frame spectroscopy uses $\mathbf{B}_1$ field of the surface coils for localization. Methods like depth resolved spectroscopy (DRESS) use $\mathbf{B}_0$ magnetic field gradients and a frequency selective pulse for localization and the methods that are mostly employed in clinical settings include stimulated acquisition mode (STEAM), point resolved spectroscopy (PRESS) and image guided *in vivo* spectroscopy (ISIS). These sequences acquire spectra from a single volume (SV). Currently, multivoxel spectroscopic [chemical shift imaging CSI or spectroscopic imaging (SI)] methods are also available which are used to acquire spectra from many voxels simultaneously. Since, most of these methods use MR images to guide the VOI localization and are more often termed as image guided localization methods. This section provides a brief survey of some of the early localization methods and those that are commonly used in clinical setting.

2.1 Surface Coil MRS

Ackerman *et al.*[16] reported the use of surface coils to monitor the metabolic status of skeletal muscle and brain in intact rats. Surface coil is a small circular loop of wire that is positioned adjacent (proximal) to a sample for excitation and /or detection and is positioned in such an orientation that a major component of the $\mathbf{B}_1$ field generated by the coil is orthogonal to the $\mathbf{B}_0$ field. Surface coil provides rough localization i.e. metabolites in the sample close to the coil are detected with good sensitivity, whereas metabolites far from the coil are not detected. In addition by varying the RF pulse length, spatial selectivity can be achieved. The disadvantages include extremely inhomogeneous transverse magnetic field, difficulty in assessing VOI that is below the surface and contamination of signals from extraneous tissues. For these reasons, surface coils are used with other techniques like the use of adiabatic pulses for precise localization and phased array surface coil with correction algorithm for inherent inhomogenities in the signal reception profile.

2.2 Rotating Frame Spectroscopy

Hoult[17] in 1979 proposed a localization technique called as rotating frame spectroscopy that employs gradient $\mathbf{B}_1$ fields of a transmitting surface coil for localization. $\mathbf{B}_1$ decreases with increasing distance from the coil and hence the spins (metabolites) that are close to the coil experience the largest flip angle. These spins will also experience more variation of the angle than the other spins if the duration of the RF pulse or amplitude is varied. This property is used for spatial encoding along the axis of the surface coil. The advantage of this method is that no switched $\mathbf{B}_0$ gradients are needed which is of benefit for observing the nuclei with short relaxation times. A wide variety of tissues and organs in both animal and human systems have been investigated using phosphorus nucleus[18,19]. Sodium MR spectra have also been obtained from the perfused rabbit heart with this method[20]. ^{19}F rotating frame imaging has been used to investigate the distribution of fluorine labeled metabolites in rat brain[21]. The disadvantages include curved isoflux contours of single surface coil probes, which result in the contamination of the VOI by surrounding layers of tissue. Hence there is lack of lateral discrimination, particularly when investigating localized lesions such as tumors.

2.3 Topical Magnetic Resonance

The first method among the techniques that use $\mathbf{B}_0$ magnetic field gradients for localization is topical magnetic resonance[22] (TMR). Non-linear magnetic field gradients are used to generate a spherical region of homogeneous magnetic field (commonly called the profiled field) surrounded by a magnetic field that is extremely inhomogeneous. The tissue lying within the sphere generates high-resolution NMR signals while the tissue lying outside the sphere (in the inhomogeneous magnetic field) generate excessively broadened NMR signals, which are removed by data processing. Surface coils can be used to transmit and receive the RF signals to and from the VOI. There are two main disadvantages of this technique. First, the localized TMR volume has a spatial profile that is approximately "bell shaped" along the diagonal through the centre of the localized volume[22]. Secondly for each VOI, the patient must be realigned and shimmed within the magnet so that the profiled field is concentric with the desired region of study.

2.4 Depth Resolved Spectroscopy (DRESS)

DRESS sequence shown in Fig.1 was developed by Bottomley *et al.*[23] in 1984, was arguably the first spatial localization technique employing magnetic field gradients ($\mathbf{B}_0$) and was successfully used to acquire localized ^{31}P and ^{1}H spectra from humans and animals. In this method, a single slice is excited by applying a slice selection gradient to the plane of the surface coil with a frequency selective RF excitation pulse ($\mathbf{B}_1$) to provide depth resolution. The observed volume is the intersection of the excited slice and the sensitive volume of the coil, and is approximately a thick disc. Spatial

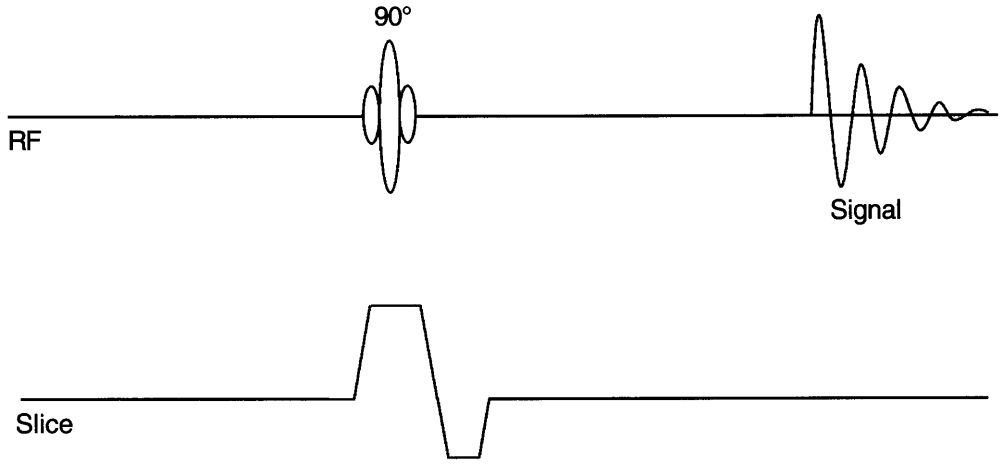

Fig. 1 The pulse sequence for DRESS. The RF excitation pulse is applied in the presence of a magnetic field gradient.

localization depends critically on the excitation pulse and the surface coil used for detection. In DRESS, the sensitivity reduces as a function of the distance from the cylindrical axis of the surface coil[23]. For observation of a deep organ, signals from the surface regions can be suppressed effectively but sensitivity of DRESS sequence is directly related to the depth of the selective pulse that poses a great limitation. Another problem with DRESS is that significant loss of signal occurs for metabolites with short T2 due to short delay of a few milliseconds between excitation and detection necessitated by the application of a gradient-refocusing lobe for acquisition.

2.5 Image Guided Volume Localization – Single Voxel (SV) Methods

MR localization methods are mostly image guided in that they use proton images to guide the placement of VOI. Hence prior to carrying out localized MRS, MR images are acquired in all the three planes and frequency selective RF pulses are applied during the application of a gradient. The magnetic field gradient spatially encodes the resonance frequencies and the frequency selective pulse excites the spin distribution within the sample. Localization techniques may be categorized as single volume (or voxel) or multivolume. The position and size of the VOI are determined by the region bounded by the intersection of the three orthogonal planes and the actual shape would normally depend on the slice profiles of the selective pulses. There are different pulse sequences available in the literature and brief details of some of the most commonly used sequences like ISIS, STEAM, PRESS, and CSI are described in some detail in subsequent sections.

2.5.1 Image Selected in vivo Spectroscopy (ISIS)

This method consists of a series of measurements having different preparation schemes for magnetization[24]. The preparation period includes selective inversion pulses (180°) that are applied in different combinations prior to collecting a FID from a non-selective 90° pulse as shown in Fig.2b. By applying selective 180° pulses in a sequence along the X, Y, and Z - axes, a cube is formed at the intersection of the selected planes that are orthogonal to X, Y, and Z – axes (Fig.2a). By varying the excitation profile width and adjustment of the individual frequency offset of each of the RF selective pulses, the size and position of the cube can be varied. Surface coil is used to obtain improved signal sensitivity. ISIS is relatively insensitive to T2 distortion and therefore most suited for *in vivo* ^{31}P spectroscopy where several metabolites have short T2 values. This is because ISIS does not produce an echo but a FID is collected right after the RF excitation. However due to the need to collect a series of acquisitions (eight for example) for localization, ISIS is more sensitive to motion artifacts. The spectrum acquired using ISIS is T1 weighted because spin-lattice relaxation occurs during the time interval between the selective inversion preparation period and the 90° RF readout pulse.

2.5.2 Stimulated Echo Acquisition Mode (STEAM)

This method shown in Fig.2c uses three frequency selective RF pulses that are applied in succession in the presence of mutually orthogonal X, Y and Z - field gradients[25,26]. The localized VOI is at the intersection of the three orthogonal slices (Fig. 2a). Each pulse is of 90°, and the second 90° pulse brings the magnetization to the longitudinal direction where it

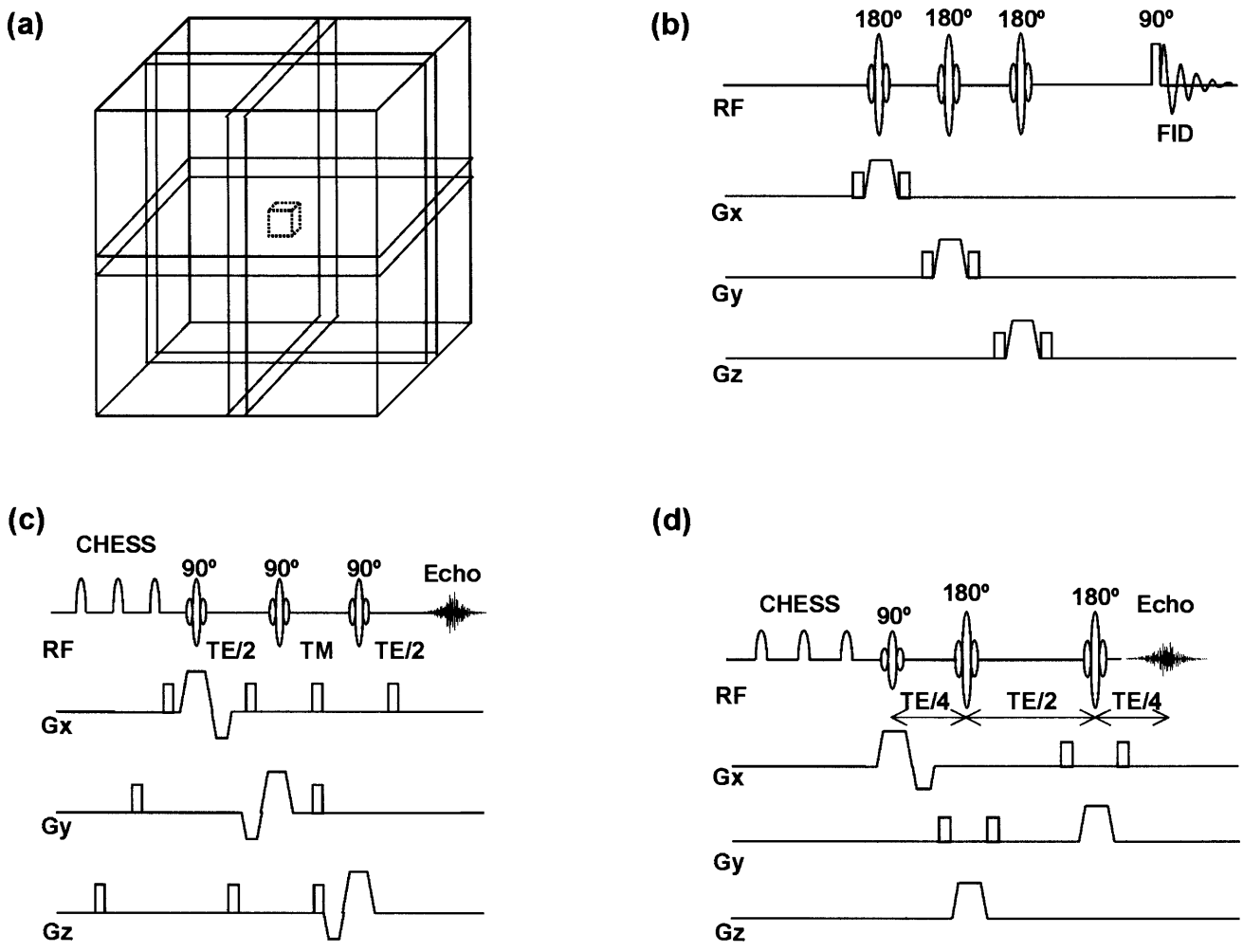

Fig. 2 (a) A voxel that is defined by the intersection of three orthogonal planes; (b) The RF and gradient pulse timings for ISIS; (c) Timing diagram of a STEAM sequence. The initial CHESS pulses are for water suppression. Here all the slice selective RF pulses are 90^0 and are applied with slice selection gradient each along one of the orthogonal directions X, Y or Z. Gradients in the sequence optimize the stimulated echo and suppress all other signals; (d) Timing diagram of a PRESS sequence. The initial CHESS pulses are to suppress the water signal. Slice-selective RF pulses excite three interacting orthogonal planes.

remains for a time period TM. In all four echo signals are formed following the last RF pulse: one at TM arises from the second and third pulses, one at (TE/2 – TM) is formed by the first and second pulses, one at (TE/2 + TM) results from the first and third pulses and the stimulated echo is formed at the end of second TE/2. Only the stimulated echo is acquired while all the unwanted echoes and the FID are suppressed using spoiler gradients. To achieve optimal efficiency each pulse should be 90°; however, it is not crucial to localization so long each of them is less than or equal to 90°. This reduces total investigation time and also since pulse angle can be less than 90°, the RF power deposition on tissues is less. However, whatever the nominal pulse angles, STEAM requires a complete dispersion of phases during the first echo delay and destruction of transverse magnetization during TM. The high quality localization obtained with STEAM has made it one of the most frequently utilized single voxel MRS technique despite the disadvantage that there is loss of a factor of two in S/N as compared to Curr-Purcell echoes. STEAM is not well suited for observation of nuclei with short T2 values like ^{31}P. In general, the T2 values for protons are much longer than the T2 values of ^{31}P, and the use of STEAM has been primarily for localized proton MRS.

2.5.3 Point Resolved Spectroscopy (PRESS)

The point resolved spectroscopy (PRESS) or double spin-echo was proposed by two groups[27,28]. Spatial localization is achieved by three frequency selective pulses applied in the presence of an orthogonal gradient

(Fig. 2d). The first 90° pulse is applied in the presence of gradient (e.g. along the X - axis) that selects a slice orthogonal to this axis. The magnetization of the selected slice is allowed to precess during TE1/4 and is refocused by a second pulse applied in the presence of a gradient along an orthogonal direction (e.g. the Y- axis). At TE1/4 it refocuses the magnetization in a slice orthogonal to this axis. Finally, after a free precession delay TE2/4, a second refocusing pulse is applied in the presence of a gradient along the direction orthogonal to the first two directions (Z - axis). This last pulse refocuses the transverse magnetization from a slice orthogonal to the first two slices. Therefore the acquired signal results from the volume element common to the three slices, producing a three-dimensional localization in one single scan. PRESS offers the important advantage of a factor of two gain in S/N, although signals are T2 weighted and J-modulated. The VOI definition and localization in PRESS are inferior to other sequences such as STEAM since the slice profiles of the 180° pulses are often worse than those of a 90° pulse. Further, the power requirement for 180° pulses is twice that of a 90° pulse, which may cause RF heating of tissues. Another disadvantage is the lengthened minimum echo time that is an important limitation for metabolites with short T2.

2.6 Multi Voxel Spectroscopy: Spectroscopic Imaging (SI)

Single voxel ^{1}H NMR spectroscopy can be extended to multivolume called chemical shift imaging (CSI) or SI[29,30]. The spatial information (encoding) is accomplished by switched gradients of the $\mathbf{B_0}$ field. The data in SI is collected in the absence of a readout gradient to preserve the chemical shift information while in MRI readout gradient is used to obtain spatial information in one of the dimensions. Similar to the phase-encoding in MRI, a sequence of gradient values generates a complete set of spectra which can be spatially and spectroscopically resolved after multidimensional FT. Spectroscopic imaging procedures can be applied for 1D, 2D or even 3D acquisition of an organ. Since, localized spectra from many locations can be acquired simultaneously; SI is a more attractive method than single voxel techniques. Fig. 3a shows the MR image of a patient suffering from glioma wherein the CSI or the VOI grid is shown as a big square while Fig.3b is the proton MR spectrum obtained from one of the voxels of CSI from the tumor region. Fig.3d shows the proton spectrum obtained from one of the voxels from the normal portion of the tissue as shown in Fig.3c. The advantages of SI include acquisition of spectral data from small VOIs and the ability to reconstruct low-resolution metabolite images from the spectral data in which the pixel intensity is proportional to the relative concentrations of the metabolites. These metabolic maps or images are useful in visually assessing the spatial variation in the metabolite concentrations. EPI-based SI sequences are now available, which decrease image acquisition times.

However, the disadvantage of SI is that the signal from a voxel is prone to contamination coming from outside the VOI. This contamination occurs due to discrete and finite sampling, since the number of phase-encoding steps is typically more limited than normal imaging acquisitions. In addition, shimming the magnetic field over large volume of tissue and long acquisition times are other disadvantages. Gradient induced eddy currents and inhomogeneity in static magnetic field makes water suppression using CHESS pulses problematic in SI and leads to individual spectra being offset in frequency.

Recently in an effort to combine the advantages of both the SV and SI localization methods, while decreasing the disadvantage of either method, an approach to acquire *in vivo* data combining both SV and SI sequences are developed. The hybrid SV-SI pulse sequences that combined STEAM SI localization of a large volume of interest is shown in Fig. 4. SV method is used to localize a relatively large VOI and phase-encoding gradients are used to subdivide the large VOI into smaller voxels. The advantage of SI localization from multiple voxels is retained, while the use of the SV method to preselect the large VOI greatly minimizes spectral bleed contamination from the outside lipid signals. The method allowed improved shimming, improved spectral resolution and water suppression. Several multidimensional experiments have demonstrated the potential of SI in the study of human brain[31-34].

3 Water Suppression and Other Considerations

In proton MRS, detection of resonances from metabolites with lower concentrations in the presence of a large water proton signal is a major problem. The concentration of water in tissues is of the order of 70M compared to the millimolar (mM) concentration of other metabolites. Hence, there is the need for water suppression from the VOI and several methods have been developed that exploit the chemical shift

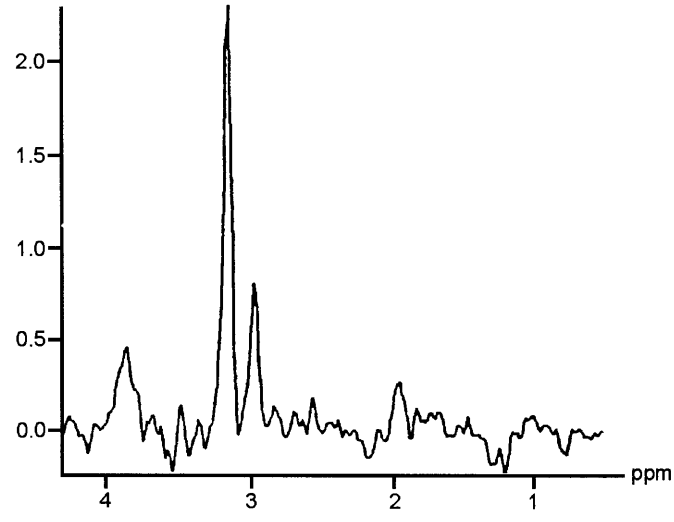

(a)

(b)

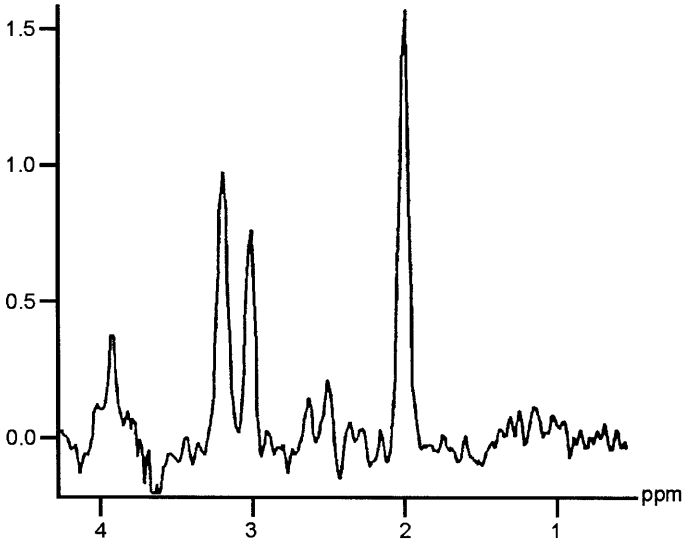

(c)

(d)

Fig. 3 (a) T1-weighted axial brain image of a patient showing the area of glioma on the right side. The CSI grid or VOI is the bigger square from which different smaller voxels of the size shown are used to get the proton MR spectrum; (b) Proton MR spectrum from a voxel from the tumor region; (c) Proton MR spectrum form a voxel which is from the normal portion of the brain; (d) The voxel location from which MRS shown in (c) was obtained.

differences between the water and the other metabolites[9-11]. The common one is to use chemical shift selective (CHESS) RF pulses[12], which excite a limited narrow band (~ 60 Hz) of RF frequencies corresponding to the water signal in the sample. In this method one or more 90° RF excitation pulses are applied at the water signal and in addition 'crusher' gradients are used to eliminate the excited water signal in the transverse plane (see Fig. 2c). The other metabolites are given the RF excitation in the selected region and detected in the period when water magnetization is beginning to recover and not available for excitation. Most commonly used techniques of *in vivo* proton MRS like STEAM and PRESS, use CHESS pulses in the beginning of the sequence for water suppression (see Figs. 2c and d).

In *in vivo* MRS, often the spin echo signal is collected. STEAM and PRESS require the use of long echo times of 135 to 270 ms for adequate water suppression and to avoid instrumental problems, such as eddy currents due to the application of the magnetic field gradients for localization. Such long delay between the excitation and acquisition often results in dephasing the signals of the metabolites due to T2 relaxation. For

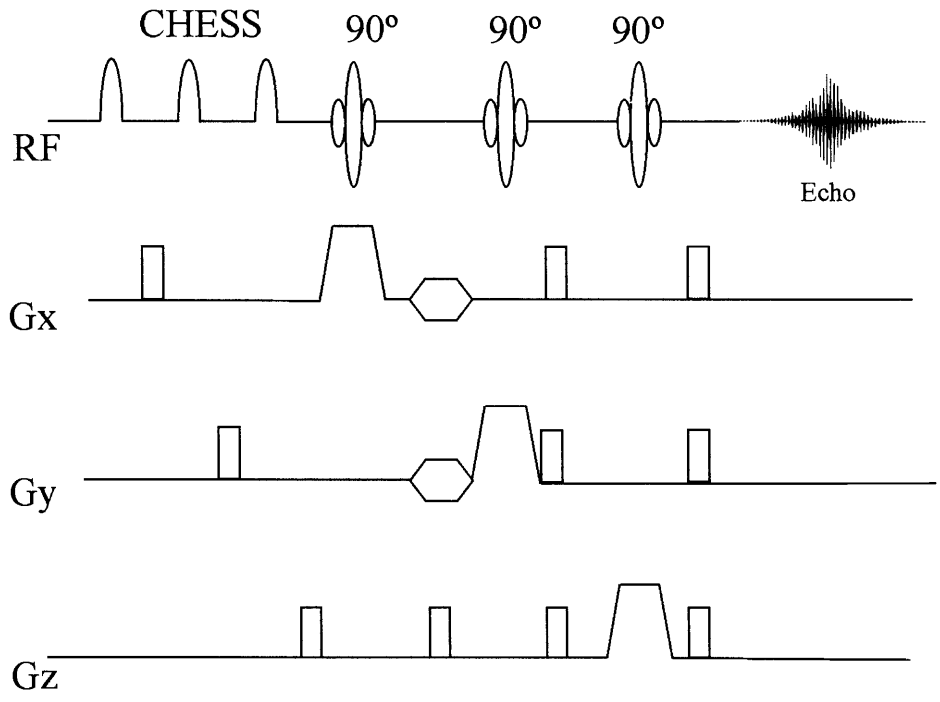

Fig. 4 Sequence diagram for hybrid spectroscopic imaging (SI) and single voxel (SV) technique that combines STEAM SV localization of a large VOI and 2-dimensional SI

metabolites with short T2 this can lead to almost complete loss of the signal. Therefore, the choice of TE in localization sequences is important for observing the metabolites of interest. The methylene protons of glutamate (Glu) and glutamine (Gln) are observed as complex multiplets at short TE's due to J- modulation[35]. To observe the methyl resonances of lactate (Lac) and alanine (Ala) often-longer TE's such as 135 and 270 ms are used to allow the signals to rephase. To observe metabolites like GABA and lactate, spectral editing techniques are sometimes used (*vide infra*). For TE's greater than two or three T2 intervals (e.g. mobile lipids), the use of shorter TE's can reduce the signal loss. In ^{31}P MRS since T2 of most of the phosphorus containing compounds are short, measurement of free induction signal is preferred to avoid the loss of metabolite signal.

4 Clinical Applications of *in vivo* MRS

Over the past decade *in vivo* MRS has increasingly been applied in clinical setup using nuclei like ^{1}H and ^{31}P to study the metabolism of several disease processes. It will not be possible to review all such studies that appeared till date, however a brief survey of the application of MRS in brain, muscle and breast are presented in this article with examples of the work carried out in our laboratory. In addition, the potential of few other nuclei in studying the tissue metabolism is also outlined.

4.1 Phosphorus MRS

^{31}P is the naturally occurring nucleus that has been most extensively used for studying *in vivo* tissue energetics and the spectra are simple to comprehend since the MR signals are observed only from the relatively mobile compounds, which are in mM concentration. Thus, monitoring the relative concentration of various ^{31}P metabolites noninvasively helps to study the biochemistry of diseased and normal states of tissues and can also be used to monitor the efficacy of several therapeutic interventions. The first observation was made in 1974 on an isolated, intact rat muscle which demonstrated that ^{31}P NMR can be used noninvasively for determining the intracellular pH and for probing the intracellular concentration of metabolites, interaction and reaction rates[36]. Fig. 5a shows the ^{31}P MR spectrum from the human calf muscle of a volunteer recorded in our laboratory. The spectrum shows resonances from β-adenosine-tri-phosphate (ATP), at –16 ppm, signal at –2.5 ppm is characteristic of γ-ATP while the signal at –7.5 ppm contains contributions from the α- phosphate groups of both ATP and adenosine – di – phosphate (ADP). The resonances at 0 and 5 ppm are due to phosphocreatine (PCr) and inorganic phosphate (Pi), respectively.

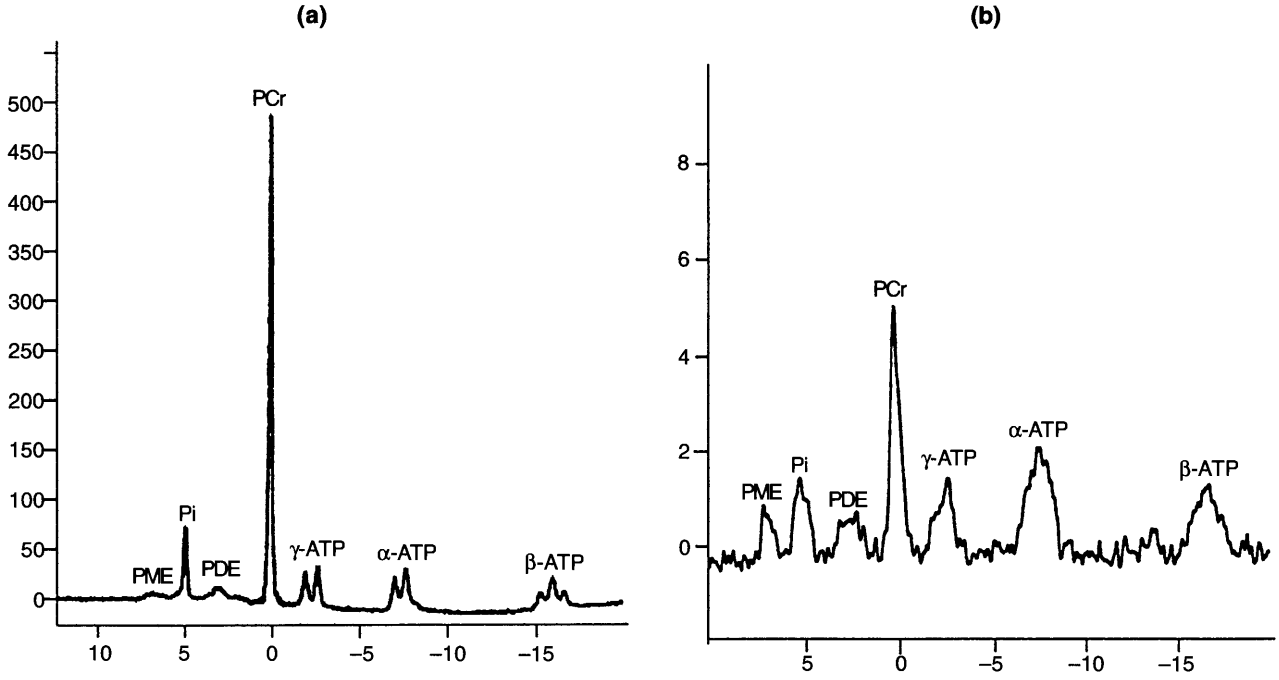

Fig. 5 (a) ^{31}P MR spectrum from the left calf muscle of a volunteer using a surface coil. A single RF pulse was used for excitation with a repetition time of 3s; (b) ^{31}P MR spectrum from the left calf muscle of a post-polio residual paralysis patient who had severe impairment of both the lower limbs. A single RF pulse was used for excitation with a repetition time of 3s

The chemical shift position of Pi is sensitive to pH and provides a noninvasive indicator of intracellular pH. Considering PCr as a reference peak, changes in Pi peak are measured. Pi peak shifts to the right with acidic change in pH while alkaline change in pH shifts the peak to the left. Besides Pi, ATP and PCr, signals from phosphomonoesters (PME; 6 - 8 ppm) and phosphodiesters (PDE; 2 - 4 ppm) are also observed. The PME peak contains several compounds such as sugar phosphates and phosphocholine (PC). The metabolic state of cells can thus be studied by monitoring the PME peak. Increase in PME in malignant cells suggests alterations in lipid metabolism[37,38]. Glycerophosphocholine (GPC) and phosphoethanol amine (PE) are major PDE components observed in ^{31}P spectra and the importance of these metabolites has been discussed elsewhere[39]. The chemical shift positions of the β and γ phosphates can also be used to obtain information whether ATP is complexed to divalent metal ions like Mg^{2+}.

4.1.1 ^{31}P MRS of Brain

Large number of papers has shown that *in vivo* ^{31}P MRS can be used as a diagnostic tool to monitor the metabolic changes of several disease processes that affect brain[40]. The ^{31}P spectra of normal newborn human infants showed high PME[41,42]. Decreased PME/PDE ratio was observed during the first six months of life with a significant increase in PCr/ATP and variation in NAD[43]. Studies have shown that birth asphyxia complications of premature birth, birth trauma and other insults to infants produce detectable changes in brain metabolites. The PCr/Pi ratio was suggested to be a good prognostic indicator of the likely clinical outcome following asphyxia. In focal cerebral ischemia, change in the pH with respect to the levels of ^{31}P metabolites has been documented[44]. Recently, Jensen *et al.* used ^{31}P 3D CSI to determine the *in vivo* concentrations of phosphorus containing metabolites in the brain[45].

Fig. 6 shows the phosphate metabolites that are observable in the brain from the occipital region of the brain of a normal volunteer recorded in our laboratory using a surface coil. Significant differences between normal and brain tumor tissues have been reported using ^{31}P MRS by a number of investigators. Reduction in PCr and PDE with increased PME peaks was reported in meningiomas, while malignant gliomas showed less distinct changes[40]. In brain tumors, Hubesch *et al.*[46] have shown that ^{31}P metabolites are reduced to 20 % to 70 %. PME, PDE and PCr showed the greatest changes while Pi showed the minimal change. Segebarth *et al.* reported that tumors (prolactinoma, lymphoma) showed high PME while radiation and

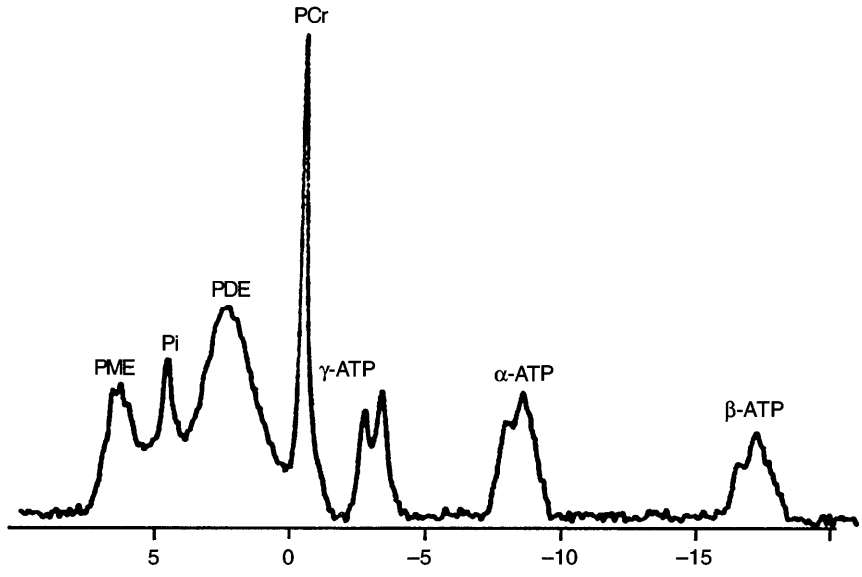

Fig. 6 ^{31}P MR spectrum form the occipital lobe of the brain of a volunteer obtained using a surface coil. A single RF pulse was used with a repetition time of 3s

chemotherapy treatment caused reduction in PME[47]. Maintz *et al.* compared localized ^{31}P spectra of normal brain with brain tumors [gliomas (grade I and II)], glioblastomas and meningiomas[48]. In meningiomas, alkaline pH and decrease in PCr and PDE metabolites was reported. Glioblastomas also showed alkalization and a decrease in PDE/α-NTP but no significant changes in PCr/ α-NTP or PCr/Pi ratios. In low-grade gliomas, less distinct changes were detected with slight alkalization and more than a two-fold reduction in the PDE/α-NTP ratio.

^{31}P MRS has also been used to follow patients with recurrent mixed astrocytoma/ oligodendroglioma treated with intra-arterial BCNU at 6-week intervals. Prior to treatment PDE was 25% less than the normal and intracellular pH was 7.14. After 8 hrs, PCr and PDE were reduced by about 40% and pH increased to 7.24 while after thirty two hours, PCr and PDE increased further and the pH increased to 7.35. This study demonstrated that ^{31}P MRS could detect chemical changes in a tumor shortly after chemotherapy[49].

4.1.2 ^{31}P MRS of Muscle

Many research groups have carried out sequential ^{31}P MRS to investigate the changes in muscle metabolism at rest and during exercise and recovery. In addition, investigations of various neuromuscular diseases have also been recently reviewed[50-52]. Studies on human muscle usually employ a surface coil for recording the spectra. In normal exercising muscle the concentration of ATP remains constant while PCr falls, and that of Pi produced by ATP hydrolysis is stochiometrically increased[50]. Intense exercise produce severe intracellular acidosis (pH < 6) and acute changes in muscle pH, presumably reflecting a balance between early proton consumption by PCr hydrolysis and lactate production by glycolysis[50]. During recovery PCr gradually increases while Pi and ADP decreases, and the pH returns to its rest level. Relationship between work and oxidative phosphorylation has also been investigated in human muscle. During moderate exercise a linear relationship between the work rate and the Pi/PCr ratio was observed suggesting that the ADP levels regulate the oxygen consumption. Biochemical changes underlying muscle fatigue has also been reported in several studies[53]. Muarer *et al.* examined muscle metabolism in professional atheletes[54]. Sprinters displayed a higher PCr/Pi and PCr/β-ATP ratio than marathon runners, while for middle distance runners these values were in between. Kutsuzawa *et al.* studied the effect of aging on muscle metabolism and reported that PCr/(PCr+Pi) and pH at rest and after the completion of the exercise did not differ between young and older subjects[55]. In chronic malnutrition, the levels of PCr/ATP at rest in the muscle are reported to be reduced[56,57].

^{31}P MRS has also been increasingly used for diagnosis and monitoring of mitochondrial diseases. The level of PCr/Pi at rest was reported to be abnormally low in mitochondrial myopathy[50]. Patients with McArdle's disease show a paradoxical increase in

muscle pH because of the consumption of protons associated with PCr hydrolysis[58]. Furthermore, ^{31}P MRS is also useful in discriminating disorders of glycogenolysis (McArdle's disease) and glycolysis[50,59]. A high intracellular pH and reduction in the level of PCr at rest has also been reported in the muscle of patients with muscular dystrophy[50,60,61]. In patients with Becker's dystrophy[62,63] and carriers[60,64], during exercise a premature drop in PCr levels (or PCr/Pi) and reduced acidosis was reported. Lodi *et al.* suggested that reduced cytosolic acidification during exercise in patients with BMD may be due to deficit in glycolytic lactate production in patients[63]. Felber *et al.* reported that oral creatine supplementation improve the muscle performance in DMD patients[65]. Fig. 5b shows the representative ^{31}P MR spectrum recorded in our laboratory using a surface coil from the calf muscle of a polio patient who had severe impairment (90%). Statistically significant reduction in all the phosphorus metabolites was observed in polio patients compared to that observed for healthy controls (see Fig. 5a). ^{31}P MR studies have also been carried out on inflammatory disorders by Park *et al.*[66,67]. High Pi/PCr ratio at rest and larger depletion of PCr/Pi in patients with dermatomyositis was noticed. Recently, Cea *et al.* reported that the rate of ATP production and recovery times for PCr and ADP are almost twice in patients with polymyositis and dermatomyositis as compared to controls suggesting impaired aerobic function[68]. However, no correlation was observed between the MRS detected abnormalities and the degree of inflammation or fatty infiltration shown by MRI.

4.1.3 ^{31}P MRS of Breast

Several studies have been reported on the normal and breast cancer tissues. Ronen and Leach[69,70] reviewed the results of ^{31}P MRS on breast cancer using patients while the phospholipid metabolism in breast cancer patients was reviewed by Podo[40]. In the normal breast tissues PME was lower, while the PDE/PME ratio was higher during the second week than at the other stages of the menstrual cycle[71]. PME was also seen to be increased in the lactating breast by a factor of two compared to the non-lactating premenstrual breast[40]. In general, the phosphate metabolites were lower in the post-menopausal women compared to the pre-menopausal women. Using ISIS localization, Payne *et al.* studied the normal breast tissues and observed higher level of PME at the late follicular (LF) phase of the menstrual cycle compared to the early luteal (EL) phase while PDE was maximum at the early EF phase compared to the LF phase[72]. Significant changes in PME were noticed compared to that observed in PDE. Higher PME in human breast tumors has been demonstrated by a number of investigators using *in vivo* methods[73-75] conditions. In excised breast carcinoma in culture medium the content of PME and NTP was three times higher than in benign breast lesions[76]. Ng *et al.* reported higher total phosphate level in breast carcinomas compared to the normal breast from non-menstruating women[77]. In untreated human breast tumors PME was found to be higher than in the spectra of normal breast of post-menopausal women.

4.2 Proton MR Spectroscopy

Proton has the advantage of having the highest sensitivity, 100 % natural abundance and is present in all biologically important metabolites, and hence useful to study noninvasively the tissue metabolism. However, there are major technical problems associated with ^{1}H MRS since there is a need to suppress water signal, which are several hundreds of times higher in magnitude than the metabolites of interest. However, with the development of techniques of water suppression and spectral editing[1-3,6-8], ^{1}H MRS is now being routinely employed to study the biochemistry of brain, muscle, breast and other organs.

Fig. 7 is the proton MR spectrum recorded from the fronto-partietal region of the brain of a normal volunteer. The strong peak at 2.02 ppm corresponds to N-acetyl group of NAA and is evenly distributed through out the cerebral cortex. A small fraction of N-acetyl aspartyl-glutamate (NAAG), a neuromodulator or neurotransmitter also contributes to this signal[78]. As per the prevailing concept, NAA is considered as a neuronal marker or oligodendrocyte precursor[79-81]. Non-cerebral tumors show little or no NAA[82]. However, some studies reported NAA in other cells[83]. The concentration of NAA is likely to reduce in diseases that selectively cause neuronal loss (Table-II).

The $N(CH_3)$ group of creatine/ phosphocreatine (Cr/PCr) appears as a strong signal at 3.03 ppm. Minor contributions to the intensity of this peak may come from GABA, lysine, and glutathione, which are observed only by using editing sequences[84,85]. The peak from $N\text{-}CH_2$ of Cr may be visible at 3.94 ppm. Although Cr is of little biochemical interest, the equilibrium enzyme creatine kinase (conversion of Cr to PCr) appears to be crucial to the maintenance of energy-dependent systems in all the brain cells. PCr serves as

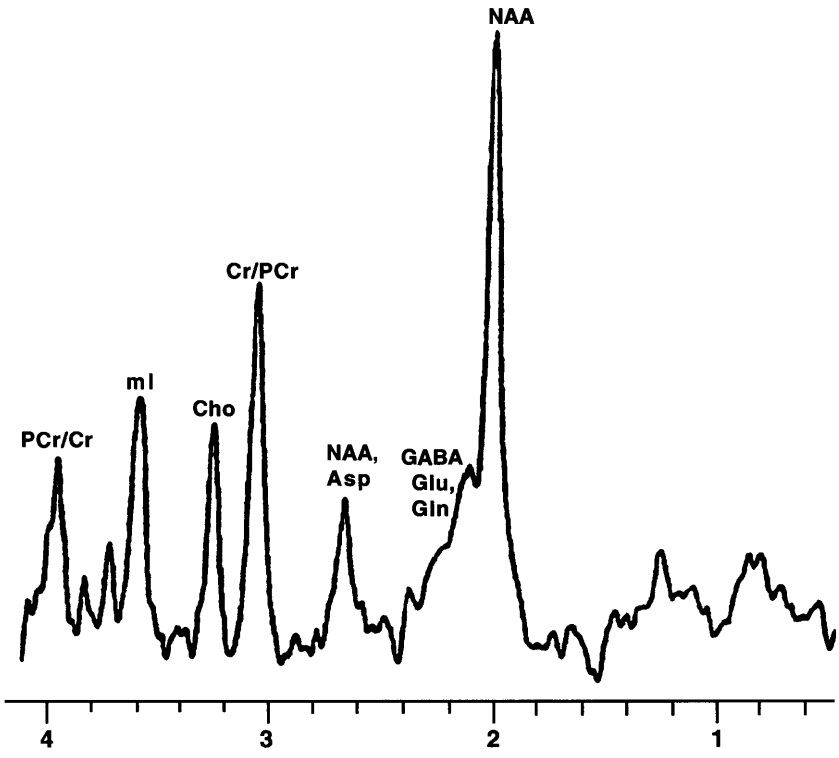

Fig. 7 Water suppressed proton MR spectrum from an 20 x 20 x 20 mm^3 voxel acquired from the fronto-parietal region of the normal brain of a volunteer obtained using STEAM pulse sequence at an echo time of 20 ms with a repetition time of 3s and the number of averages accumulated 256

Table - II

Concentration of Some Brain Metabolites in Normal and Diseased Conditions

Metabolite	Increased (↑)	Decreased (↓)
N-Acetyl-aspartate (NAA) (normal 7-15mM)	Axonal recovery e.g. MS; infant development; Hyperosmolar states; Canavan's; post head injury.	Hypoxia; anoxia; ischemia; Alzheimer's and other dementia; developmental delay; epilepsy; MS; neoplasm; stroke; PML; lymphoma; tumor; SIADH; encephalitis; diabetes mellitus; Alexander's; AIDS/HIV; head trauma; toxoplasmosis
Creatine (Cr) (normal 4-5 mM)	Trauma (Hyperosmolar response); increase with age.	Hypoxia; stroke; tumor; infant; trauma; lymphoma; hyponatremia; PML; toxoplasmosis; SIADH
Choline (Cho) (normal 1-2 mM)	Trauma; diabetes; neonates; post liver transplant; tumor; chronic hypoxia; stroke; post liver transplant; Hyperosmolar.	Asymptomatic liver disease; HE; toxoplasmosis; nonspecific dementia; hyponatremia; cryptococcoma; SIADH
Lactate (Lac) (normally less then 1 mM)	Hypoxia; anoxia; ICH; near-drowning; stroke; Canavan's; Alexander's; hydrocephalus; lymphoma; toxoplasmosis.	
Lipids (Lip)	Lymphoma; cryptococcoma; active growing tumor; PML; toxoplasmosis; MS; inflammatory diseases; toxoplasmosis	
myo-inositol (mI) (normally 5 mm)	Alzheimer's Diabetes mellitus Hyperosmolar states; Neonate PML	Chronic HE Stroke; toxoplasmosis Tumor Lymphoma Hypoxic encephalopathy
Glutamate (Glu; ~ 10 mM) Glutamine (Gln; ~ 5 mM)	Chronic HE; hypoxia; Near-drowning	Hyponatremia; post-trauma; SIADH; possible Alzheimer's disease
Glucose (Glc; ~ 1 mM)	Diabetes mellitus; HE ?	

HE: hepatic encephalopathy, ICH: intracranial hemorrhage, MS: multiple sclerosis, PML: progressive multifocal leukoencephalopathy; SIADH: syndrome of inappropriate antidiuretic hormone secretion

a reserve for high-energy phosphates and as a buffer to ATP and ADP reservoir[81]. Cr also functions as an osmolyte responding to osmotic (Donnan) forces. Thus, Cr is increased in hypermetabolic and hyperosmolar states and decreased in hypermetabolic and hypoosmolar states[86].

Another important metabolite observed in the brain spectrum is choline (Cho). The $N(CH_3)$ group of Cho exhibits a strong signal at 3.22 ppm, which has contributions from other choline-containing compound such as GPC, PC and PCho. All these are components of phospholipid metabolism of cell membranes[87] and hence increased Cho may reflect increased membrane synthesis[88]. Cho is also involved in the synthesis of neurotransmitter acetylcholine and phospholipids. Cho level increases in many solid tumors and high-grade solid gliomas generally have higher Cho than low-grade solid tumors.

In normal brain the concentration of Lac is very less and its presence therefore, suggests that normal cellular oxidative respiration mechanism is no longer in effect and energy is derived via anaerobic glycolytic activity[89]. The methyl protons of Lac appear as a doublet at 1.33 ppm. Although its identification and measurement is difficult in *in vivo* MRS due to the presence of the strong lipid peak at 1.3 ppm, its assignment can be made by exploiting the phase modulation in a spin-echo experiment. By keeping TE equal to 1/J (J = 7 Hz), spectra can be obtained in which CH_3 lactate resonance is inverted[90]. This period approximately corresponds to the frequently used TE of 135 ms and it is refocused at 270 ms. Several editing methods, such as double quantum coherence filtering[91] and spin echo difference using selective decoupling, selective inversion[90,92] or zero quantum are used to eliminate the overlapping of Lac resonance with lipid and water.

Glu and Gln resonances appear as broad peaks between 2.1 and 2.5 ppm in the *in vivo* ^{1}H MR spectrum and are normally detected at short TE. Glu is the most abundant of the amino acids in the brain and acts as excitatory neurotransmitter. Glu metabolism is related to the determination of the steady-state concentration of many other metabolites, including the mitochondrial redox state (NAD/NADH) of the cell and the so-called malate:aspartate shuttle. Two important products of Glu metabolism are Gln, formed by transamination of Glu (this reaction uses ammonia) and GABA, formed by decarboxylation of Glu[93]. Gln is probably important in the detoxification and regulation of neurotransmitter activities of its precursor Glu; while GABA is an inhibitory neurotransmitter. In various neurologic disorders such as cerebral stroke, prolonged seizures, neurodegenerative disorders, hypoglycemia and mitochondrial encephalopathy, a disturbance of the normal Glu–Gln regulatory metabolism has been suggested to be present[94].

The peak due to myo-inositol (mI) appears at 3.56 ppm is a control metabolite in neural function and has been suggested as a possible degradation product of myelin and a marker of glial cells[95]. A triphosphorylated derivative of mI is believed to act as a second messenger of intracellular calcium mobilizing hormones[96]. MI has been found to be increased in patients with Alzheimer's[97], diabetes[98] and hepatic encephalopathy (HE)[99].

In addition, resonances due to glucose (Glc; at 3.43 and 3.50 ppm) can also be observed in proton MRS of brain. The direct observation of Glc however, is hampered by the water signal as well as due to the overlap with from taurine, mI, Glu and Gln resonances. Measurement of Glc by using ultra shot echo STEAM method has been suggested by Tkac *et al.*[100]. Resonances due to lipids are observed at 0.8, 1.2, 1.5 and 5.3 ppm that are due to the methyl, methylene, allelic the vinyl protons of the unsaturated fatty acids. Membrane lipids generally have very short relaxation times in brain and are not normally observed at long TE's. Lipids may be increased in high-grade astrocytomas and meningiomas and may reflect necrotic processes[101]. Table-II presents the different metabolites observed in brain under normal and diseased conditions.

4.2.1 ^{1}H MRS of Brain

^{1}H MRS has been extensively used in evaluating several brain pathologies that has been reviewed in several articles[102-104] and books[1-3,6-8]. Inter-hemispherical differences in the distribution of metabolites like NAA, Cr and Cho in normal brain have been reported[105,106]. Studies have shown that proton MRS distinguishes the normal brain tissue from tumors[102-104]. Typical proton MRS characteristics of astrocytoma are significant reduction in NAA, elevation in Cho and modest reduction in Cr[107,108]. Fig. 8 shows the proton MR spectrum of a patient suffering from glioblastoma (grade IV) recorded at an echo time of 270 ms using a PRESS sequence. High level of Cho and the presence of Lac with reduced Cr and NAA are clearly seen. Proton MRS also plays a crucial role

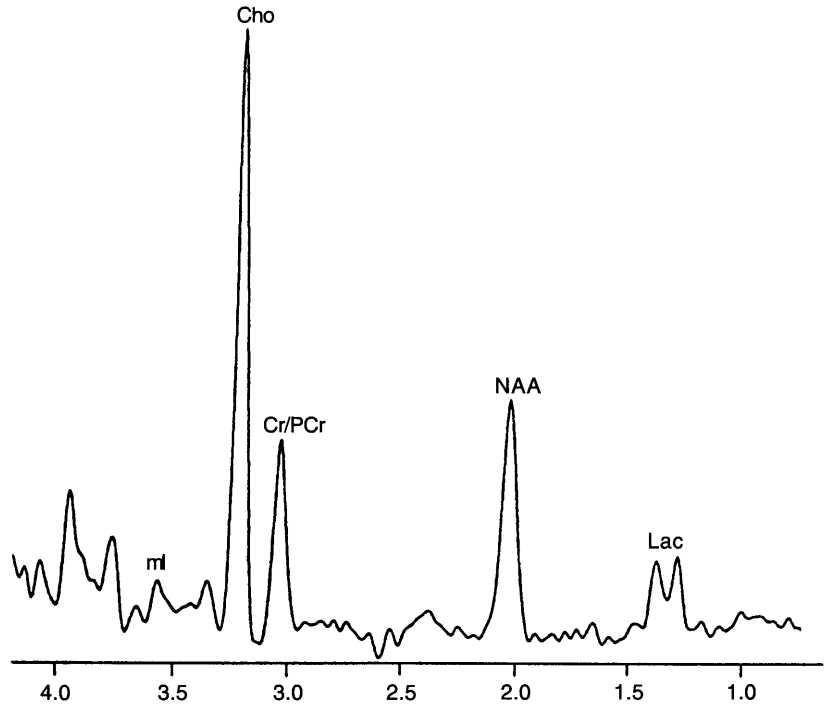

Fig. 8 Water suppressed proton MR spectrum from an 20 × 20 × 20 mm^3 voxel of a patient suffering from glioblastoma (grade IV) recorded using PRESS sequence at an echo time of 270 ms with a repetition time of 2 s

in monitoring the response of treatment of disease processes and differentiating the recurrence of tumors from post treatment effects. Sijens *et al.* reported that although proton MRS is not suited to recognize the primary tumor metastasis, could serve as a clinical test for excluding (metastatic) tumor as a cause of solitary focal brain disorders that are hard to diagnose with current imaging methods[109]. Recently Hartmann *et al.* documented that metastases have elevated Cho similar to anaplastic astrocytomas, but can be differentiated from high-grade gliomas by their higher lipid levels[110]. Ishimaru *et al.* used proton MRS in differentiating high-grade gliomas from metastases[111]. All the tumors exhibited a strong Cho peak while 21 of metastases out of 25 showed no definite Cr peak. Absence or reduction of Cr was suggested to be indicative of metastases. Presence of lipid is indicative of cellular necrosis in glioblastoma and metastasis and absence of lipid signal may exclude metastases. Law *et al.* used spectroscopic imaging and perfusion MRI to differentiate high-grade primary gliomas and solitary metastases[112]. Elevated Cho levels were found in the peritumoral region of gliomas but not in metastases. Herminghus *et al.* performed single voxel proton MR spectroscopy on 101 patients with neuroepithelial brain tumors[113]. It was documented that Cho could provide a novel and noninvasive assessment of the proliferative activity of neuroepithelial brain tumors. Hence, the potential indications for the clinical application of ^1H MRS are grading tumors presurgically, early detection of anaplastic transformation and monitoring the treatment procedure[113].

A marked increase in Cho is also observed in meningiomas[109] and elevated Lac and Ala has also been noticed in some meningiomas[107]. A possible explanation for increased Ala in meningiomas may be due to pyruvate kinase, which is inhibited by L-alanine, resulting in an increased pool of pyruvate, which is later, converted to alanine[114]. Lymphomas show elevated Cho and lipids and reduction in Cr and NAA[115]. Increased levels of Cho and lipids may be related to an increased turn over of membrane components in activated lymphocytes and to the presence of numerous macrophages containing cellular debris. Progressive reduction of Cho and lipids following treatment and its return to normal levels was observed for lymphomas[115]. Radiation injury can also be evaluated by ^1H MRS. Elevation of brain Lac levels were observed in patients who received more than 40 Gy[116]. Other radiation changes include reduced levels of NAA, Cho and Cr that correlated with tissue death. Recently, Tarnwski *et al.* reported *in vivo* proton MRS on patients with malignant glioma before and after radiotherapy treatment and surgery[117]. After brain tumor surgery, a

significant decrease in the NAA/Cr ratio and increase in the Cho/Cr, Cho/NAA and mI/Cr ratios were documented. In addition, lactate and lipids were also observed in the spectrum. Survival correlated strongly with tumor grade and Lac/NAA ratio was suggested to be strongest prognostic factor.

In case of hyperacute stroke that affects many people, a rapid noninvasive diagnostic test is desirable to decide on the early treatment protocols. The first visible change in the ^{1}H MRS after the onset of ischemia is the appearance of lactate[118]. Decreased NAA can be seen within 30 to 60 minutes of induced cerebral infraction[119]. Changes in the Cho and Cr concentration during acute infraction seem to be more variable than changes in Lac and NAA[119]. Sub-acute and chronic stages show progressive decreases in NAA, Cr and Cho[120]. Graham *et al.* reported that macromolecule signals were elevated in stroke relative to normal brain and tend to increase in the subacute period even as Lac peak declined[121]. Elevated Lac levels without changes in NAA or Cho suggest the area of ischemic penumbra. Recently, using diffusion imaging and MR spectroscopy Gupta *et al.* showed that both ADC and Cho are related to glioma cell density[122]. ^{1}H MRS has also been used to evaluate cerebral abscesses that revealed low Cho (sometimes absent) and Cr levels with decreased NAA[123]. High Cho levels along with the presence of lipid/lactate are reported in benign infective/inflammatory lesions (one case each of tuberculoma, fungal granuloma and xanthogranuloma)[124]. Intracranial lesions, tuberculomas, neurocysticercosis and nonspecific inflammatory showed significant differences in NAA/Cr, NAA/Cr and Cr/Cho ratios. Lipids were seen in 86 % of tuberculomas[125].

Local temperature in tumors, in addition to influencing a number of normal biological functions such as the protein activity, enzyme mediated reactions, hemoglobin's affinity for oxygen, etc. are also known to play an important role[126]. MRS is an ideal technique to determine the local temperature of tumors noninvasively. For example, even small variations in brain temperature can affect the extent of injury in brain ischemia[127]. Knowledge of local temperature, therefore, could provide additional information on the pathophysiology of the disease processes to the clinicians. Recently few papers have described the role of proton MRS to measure tissue pH[128-130].

In addition, *in vivo* MRS is also useful in many disease processes where molecular level changes may occur much earlier than structural changes seen in MRI. We have recently used *in vivo* ^{1}H MRS to assess the effect of alcoholism in frontal lobe, cerebellum and thalamus regions of brain in alcoholic patients[131]. The MR images of these patients revealed no structural changes, however, the proton spectra were characterized by a reduced NAA/Cho and NAA/Cr ratios relative to age matched controls. Reduction in NAA was consistent with neuronal loss while reduction in Cho is suggestive of significant changes in the membrane lipids of alcoholics. Similarly, reversal of abnormalities of myelination by thyroxine therapy in congenital hypothyroidism was also demonstrated by using proton MRS while MR imaging revealed no abnormality. Biochemical changes in different regions of brain in three patients with congenital hypothyroidism before and after thyroxine therapy was documented using in *vivo* ^{1}H MRS[132]. An abnormal lipid peak that disappeared with thyroxin therapy was observed in cerebellum and frontal lobe in one patient. Significant reduction of NAA/Cr and elevation of Cho/Cr ratios in comparison to controls were documented in all three patients, which tended to normalize with thyroxin therapy.

MR spectroscopy has also been applied in studying cerebral biochemistry in several neuropschichiatric disorders[133,134]. Reduced NAA in the temporal and cerebellum regions have been reported in individuals with autism[133,134]. Auer *et al.* reported that NAA in the thalamic region was significantly reduced in schizophrenic patients, whereas Cho and mI were significantly increased in white parietal matter[135]. White matter Cr was significantly elevated in patients and correlated positively with the brief psychiatric rating scores[135]. MR imaging and *in vivo* proton MRS has been performed on the brain of 16 neonates with hypoxic ischemic encephalopathy (HIE)[136]. It was reported that MRS was more sensitive than imaging in detecting the insult due to HIE and increased concentration of α-Glx/Cr and Gly/Cr correlated better with severity of the HIE.

^{1}H MRS has also been used in the study of several neurodegenerative diseases in older adults. In patients with Alzheimer, decrease in NAA and elevated levels of mI[137-139] and Cho [140-142] have been reported. Proton MRS of basal ganglia in Wilson's disease has also been reported[143]. Biochemical changes associated with seizures and epilepsies have also been studied. Most of these studies reported decrease in NAA and NAA/Cr ratio or in the NAA and NAA/(Cho+Cr) ratio[144,145],

while others have reported only low concentration of NAA and no changes in the levels of Cr and Cho[146,147]. Increase in Cr and Cho have also been reported[145,148]. Elevated levels of Lac were also observed in some of patients with seizure[149]. Spectra recorded at low echo times provide information on intra-cerebral concentration of multiple neurotransmitters, including GABA, Glu and Gln[150]. Studies on patients treated with anticonvulsant vigabratin (GABA transaminase inhibitor) demonstrated increase in the GABA levels[151]. In patients with AIDS dementia, reduction of NAA and decreased NAA/Cho and NAA/Cr ratios were observed. In patients with low CD-4 lymphocyte counts and abnormal MR imaging of the brain, the Cho/Cr ratio is increased implying increase in choline[152]. ^{1}H MRS of newborn infected with HIV showed higher NAA/Cr and Cho/Cr ratios than those of normal controls[153].

4.2.2 ^{1}H MRS of Muscle

In recent years, volume localized proton MRS have been used by several investigators to study the processes like glycolysis and lipid metabolism in muscle[154-156]. Techniques for monitoring Lac signal in exercising muscle has also been developed[157]. Fig. 9a shows the *in vivo* proton MRS from the gastronemius muscle of a normal volunteer recorded in our laboratory. Various resonances due to residual water (at 4.7 ppm), terminal methyl of lipids (0.8-1.0 ppm), acyl chain methylene [-(CH_2) n-: 1.1 – 1.6 ppm], α- and β-methylene of the lipid chain (2-2.8 ppm) and the oleifinic protons of the polyunsaturated fatty acids (-HC=CH-: 5.5 ppm) are clearly seen. In addition, the resonances

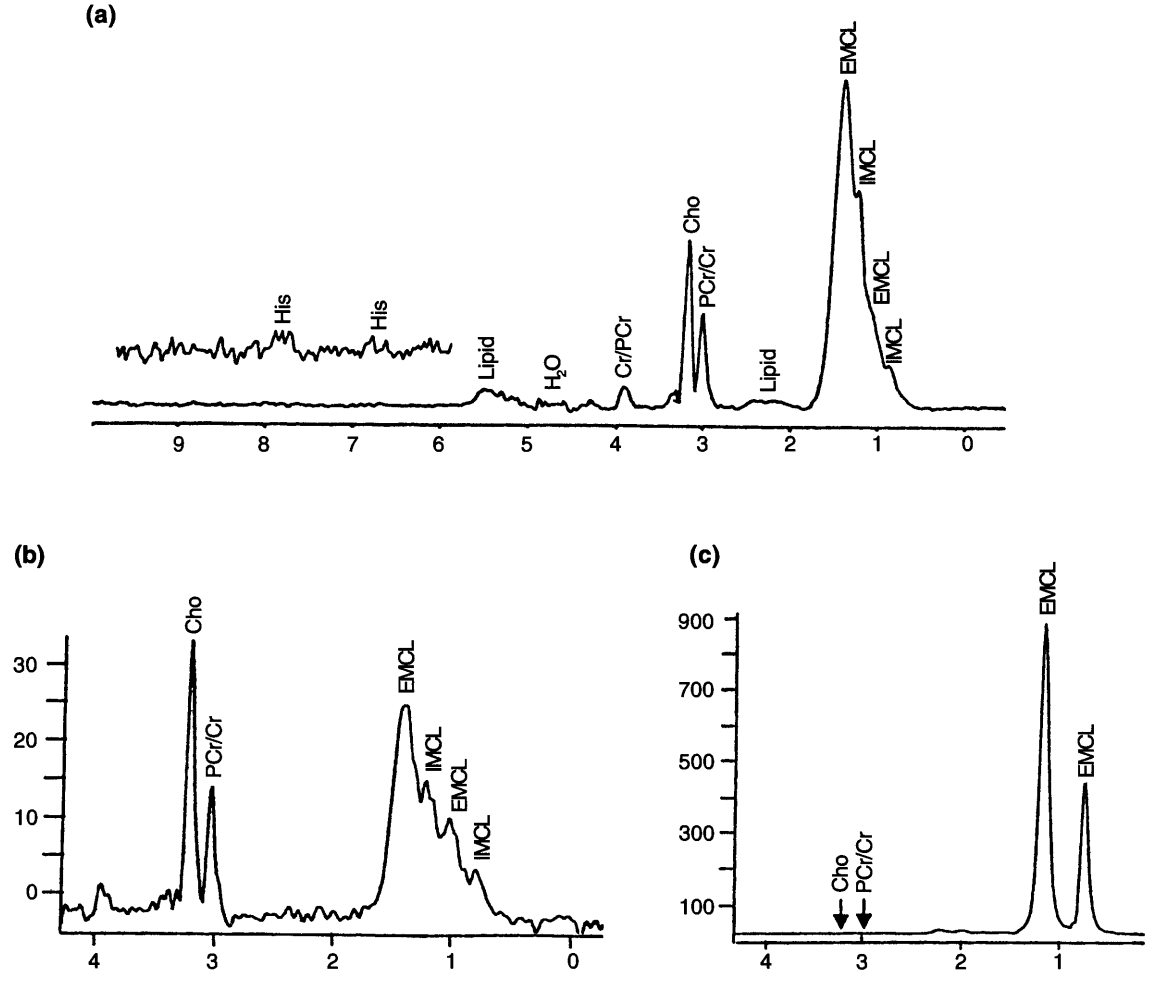

Fig. 9 (a) Proton MR spectrum form a 20 × 20 × 20 mm^3 voxel from the calf muscle of a volunteer acquired using STEAM sequence at an echo time of 135ms and a repetition time of 3 s and with 256 averages; (b) The aliphatic region of the proton MR spectrum form the same subject as in (a). The spectrum was acquired at an echo time of 270 ms to separate out clearly the different components of the lipid; (c) Aliphatic region from an 20 × 20 × 20 mm^3 voxel positioned in the calf muscle of a post-polio paralysis patient who had severe impairment of the left lower limb recorded at 270 ms echo time with a repetition time of 3s. Number of averages 64

due to N-methyl protons of Cr and PCr appear at 3.03 ppm, while the N-CH_3 of carnitine (Car) and Cho containing compounds resonate at 3.22 ppm. Peaks at 7.1 and 8.1 ppm are due to the C-4 and C-2 ring proton of histidyl moiety in carnosine. Muscle tissue being heterogeneous, spectra from different locations within the same muscle may show considerable intra-individual variation in the relative intensity of the lipid signal[155,156]. Recently Boesch *et al.* reviewed the use of ^{1}H MRS in the muscle tissue[158]. Schick *et al.* have shown that the spectra from muscle tissue exhibit two compartments of lipid signals with a difference of 0.2 ppm in their resonance frequencies[156]. These two compartments arise from intramyocellular (IMCL) and extramyocellular (EMCL) compartments of lipids. Jagannathan *et al.* demonstrated the usefulness of *in vivo* ^{1}H MRS in the study of polio patients[159]. Fig. 9a shows the aliphatic region of the proton spectrum from the calf muscle of a volunteer while Fig. 9b that of a patient who had severe post-polio paralysis of the left lower limb. The spectra were obtained at along echo time of 270 ms to characterize clearly the IMCL and EMCL components of the lipid. Our study reveled that mildly paralyzed patients are comparable with control subjects in relation to the presence of IMCL while moderate and severely paralysed patients were comparable in relation to the absence of IMCL. In addition, there is reduction or complete absence of creatine, carnitine and choline metabolites in severely paralyzed patients.

4.2.3 ^{1}H MRS of Breast

Recently, considerable interest has also been shown in the use of proton MRS methods for noninvasive detection of biochemical differences between malignant and normal breast tissues in breast cancer patients. Fig. 10 shows the MR image with voxel location and corresponding ^{1}H MR spectrum (without water suppression) from the normal breast tissue of a volunteer. The intense peaks in the spectra are at 1.33 ppm, due to methylene [-(CH_2) n-] protons of the lipid and the water peak at 4.7 ppm. The unsuppressed proton spectrum from the tumor (Fig. 11a) of a patient suffering from infiltrating duct carcinoma (IDC) is shown in Fig. 11b. The spectrum from the tumor tissue is different from the normal breast tissue and the unaffected tissue. In tumor, the water peak dominates with a much lower contribution from the protons of the fatty acid chains in comparison to the control and the unaffected breast. Comparison of water-to-fat (W/F) ratio among the above three groups showed that the tumors are characterized by high W/F values[160,161]

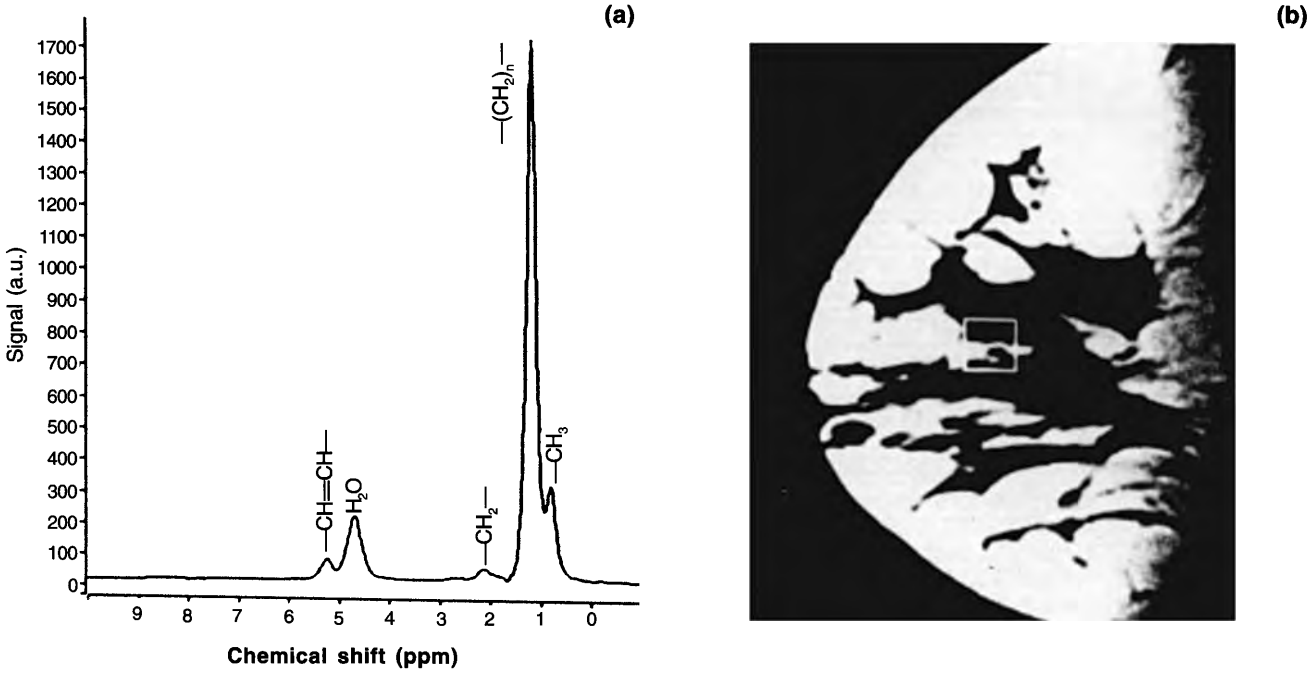

Fig. 10 (a) Proton MR spectrum from an 20 × 20 × 20 mm^3 voxel positioned in the normal breast tissue of a volunteer using STEAM pulse sequence. The spectrum was recorded at an echo time of 135 ms with a repetition time of 3s. The number of averages accumulated 32. (b) T1-weighted (TE = 15 ms and TR = 650 ms) sagittal MR image of the same patient showing the voxel location from which the proton MR spectrum was obtained

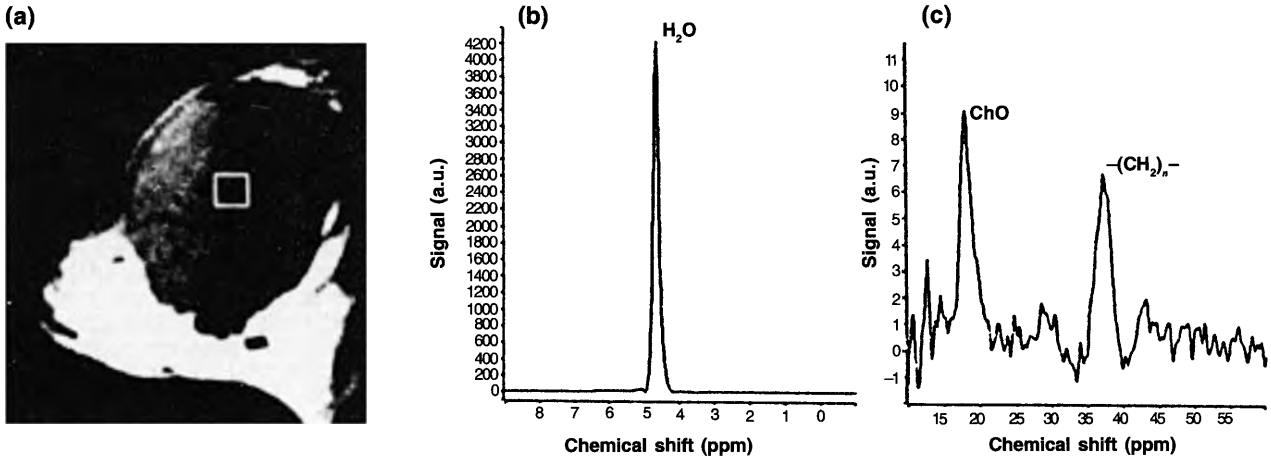

Fig. 11 (a) T1-weighted (TE = 15ms, TR = 700ms) sagittal MR image of a patient suffering from locally advanced breast cancer (IDC) showing the voxel position from which the proton MR spectrum (b) is obtained; (b) Proton MR spectrum form an 20 × 20 × 20 mm^3 voxel positioned inside the tumor a recorded using STEAM pulse sequence. The spectrum was acquired at an echo time of 135ms with 32 averages and a repetition time of 3s; (c) Proton MR spectrum as in (b) obtained with water suppression. Number of averages 64

which varied from 1 to 30, while in controls the value is 0.34 ± 0.25 and in the unaffected contralateral breast tissue of the breast cancer patients it is 0.35 ± 0.42. The observation of elevated W/F ratio observed for breast cancer patients is in agreement with the generally established trend that tumors have considerably higher water content[162]. Changes in lipid content with tumor development and progression were also reported recently by Mackinnon *et al.*[163]. The W/F ratio can also be used to monitor the efficacy of the treatment procedures in breast cancer patients[160,161]. A statistically significant reduction in the W/F ratio was noticed in patients who have undergone the full course of chemotherapy regimen (1.2 ± 1.5) compared to the pre-therapy value of 7.2 ± 7.4.

In the proton spectra with water suppression of breast cancer patients that in addition to the residual water and lipid, a peak at 3.2 ppm due to choline containing compounds as shown in Fig. 11c. The intensity of the Cho peak was monitored prior to and one week after the completion of the 3rd or 6th cycle of neoadjuvant chemotherapy for assessment of the effect of the therapy[164]. The Cho resonance was found to be either reduced or absent in patients receiving full course of chemotherapy indicating response to chemotherapy[164]. The sensitivity of *in vivo* MRS in[164] detecting Cho was 78 % and the specificity was 86 %. Similar findings have also been reported by others[165,166].

Absolute concentration of Cho in breast lesions through *in vivo* proton MRS has also been reported[167]. Mackinnon *et al.* reported elevation of Cho levels in malignant breast tumors compared to benign cases from *in vitro* NMR of FNAB samples[168]. Of the various choline-containing compounds (Cho, GPC, and PC) that contribute to the peak at 3.2 ppm in *in vivo* MRS, an increase in phosphocholine is highly probable[167,169]. Katz Brull *et al.* studied the rate of transport and metabolism of Cho in primary cultures of human mammary epithelial cells and MCF7 human breast cancer cells[170]. The rate of Cho transport under physiological Cho concentration was two fold higher in cancer cells.

4.3 Carbon (^{13}C) MRS

^{13}C isotope of carbon is also an important nucleus for studying energy metabolism. The low natural abundance (1.1 %) and poor sensitivity (1.6 % of ^{1}H) of ^{13}C some times require labelled compounds to obtain desired signal strength. It is used in a similar manner as ^{14}C being used in radioactive tracer studies. It can only be detected in storage compounds that have high intracellular carbon concentration, such as liver and muscle glycogen. The advantages are a large chemical shift range of about 200 ppm, a large number of metabolites that are well separated, and the ability to enrich substrates that are metabolized in living cells for observing chemical pathways and measuring metabolite rates *in vivo*. The compounds such as triacyl glycerols or glycogen that are carbon rich can be directly detected by ^{13}C MRS. Shulman and coworkers[171] have developed ^{13}C MR techniques for measurement of metabolic pathways. An important application of this approach was demonstrated in studies to determine

whether there was a defect in glycogen synthesis in non-insulin dependent diabetic subjects[172].

4.4 Fluorine (^{19}F) MRS

Fluorine is absent in human body and hence a perfect tracer for MR studies. Moreover, due to high signal strength (sensitivity i.e. 83 % of ^{1}H) and 100 % natural abundance makes this nucleus very appropriate for studying metabolism of fluorine containing drugs[173]. There are many drugs such as 5- fluorouracil (5-FU) and fluoropyrimidines, which are widely used in the treatment of human cancers, especially of gastrointestinal tract, breast and ovary. Metabolisms of 5-FU in animal models [174,175] and humans have been studied[176-178]. Sequential ^{19}F NMR study of breast cancer patients revealed[176] that modulators like methotrexate and levamisole of 5-FU do not significantly increase the response rate of 5-FU. ^{19}F MRS has also been used to determine the concentration levels of antipsychotic drugs such as trifluoperazine and fluphenazine and antidepressant fluoroxetine[177-179].

4.5 Lithium (^{7}Li) MRS

The isotope ^{7}Li has a spin 3/2, with a sensitivity of about 27% of ^{1}H. It typically gives a single narrow line in most biological systems arising from the Li cation in both the intracellular and extracellular environments. Lithium salts are used with considerable success in alleviating or preventing both depressive and manic recurrences of manic-depressive illness. By measuring the Li signal using *in vivo* MRS methods, pharmacokinetics and mechanism of action of Li containing drugs can be studied. Renshaw and co-workers have carried out extensive investigations on the application of ^{7}Li NMR *in vivo* spectroscopy[180]. Komoroski *et al.* followed the levels of Li in the muscle, serum and blood of a patient suffering from manic-depressive illness with an episode of hypomania[181].

4.6 Sodium (^{23}Na) and Potassium (^{39}K) MRS

There are several other nuclei that are important and provide information on several physiological, biochemical, transport and regulatory processes in biological systems. Sodium-23 (^{23}Na) and Potassium-39 (^{39}K) are quadrupolar nuclei, which can also be detected by MRS. The concentration of sodium in human, is about 44 mM. ^{23}Na has a shorter T1 relaxation time, hence experiments can be performed with short repetition times and more data averages can be acquired[182]. Sodium is the major extracellular cation while potassium is the major intracellular cation and concentration gradients of these cations across the cell membrane are maintained by the activity of the sodium-potassium activated ATPase. The concentration of ^{23}Na in intracellular compartment is very less as compared to extracellular. Differentiation between these two signals can be achieved by using paramagnetic shift reagents. ^{23}Na studies have been used to investigate membrane transport processes and the compartmentalization of sodium concentration[182]. ^{23}Na MRS has been used to discriminate between the viable and non-viable tissues in an experimental model[183]. Recently, sodium content in post-myocardial infarction in rat model has been studied[184]. ^{39}K MRS may be used noninvasively to measure alterations in K^+ homeostasis in animals and patients, perhaps to determine the effects of diuretics and other alterations[185]. The effect of K^+ uptake on the intracellular environment in rats has been reported using ^{39}K NMR[186]. Recently Redford *et al.* have used ^{39}K NMR to measure the intra cellular potassium during ischemia in the perfused guinea pig heart[187].

5 Conclusion

To day biomedical MR is experiencing a rapid expansion and has achieved amazing level of success as an important tool through MRI and *in vivo* MRS to study several disease processes in clinical and experimental research. This is due to its noninvasive nature, avoidance of ionizing radiation and its ability to generate high-resolution images. Increasing use of these methods is expected for basic research, clinical investigations and ultimately patient diagnosis. The goal of obtaining noninvasive biopsy information has pushed the development of several optimized localized MRS procedures with water suppression and editing techniques. *In vivo* MRS can now be used as a unique means to probe the biochemistry of living systems with diagnostic importance. The potentially powerful feature of *in vivo* MRS is the ability to measure endogenous metabolites noninvasively as well as changes in tissue metabolism. Besides ^{1}H and ^{31}P, there are many other nuclei like ^{19}F, ^{23}Na, ^{39}K and ^{13}C that give additional information about the biochemistry and physiology of living tissues. The technique can also be used for measuring the distribution, and pharmacokinetics of drug *in vivo*. MRS is currently employed for clinical investigation in many sites around the world, including India. The sensitivity and specificity of *in vivo* MRS for several disease patterns particularly for small lesions need to be improved before MRS can be incorporated

into clinical practice. Presently, MRS is acting as a complementary tool to histology, mammogram and other accepted techniques. However, once MRS becomes established for clinical use unambiguously in one disease, it can be expected that the available technology will be more rapidly be applied to other diseases. In fact, MRS has great clinical impact in localization of foci and brain damage in epilepsy and represents a valuable complement to conventional imaging techniques such as CT and MRI. The increased availability of 3 T and 4 T magnets would further enhance the spectral quality, particularly for proton MRS studies. The ability to perform MRI and MRS noninvasively in the same setting with the same equipment without the injection of radioactive isotopes or blood sampling provides a considerable advantage in patient care.

Acknowledgements

Dr R Jayasundar and Mr Tariq Shah are thanked for providing some of the figures presented in this article. One of the authors (US) acknowledge CSIR for Senior Research Associateship.

References

1 D Stark and W Bradley *Magnetic Resonance Imaging* New York Mosby (1998)

2 E R Danielsen and B D Ross *Magnetic Resonance Spectroscopy Diagnosis of Neurological Diseases* New York Marcel Dekker (1999)

3 N R Jagannathan *MR Imaging and Spectroscopy in Pharmaceutical and Clinical Research* New Delhi Jaypee Medical Publishers (2001)

4 P C Lauterbur *Nature* **242** (1973) 190

5 H Gunther *NMR Spectroscopy, Basic Principles, Concepts and Applications in Chemistry* New York John Wiley & Sons (1995)

6 D G Gadian *NMR and its Application to Living Systems* Oxford Clarendon (1982)

7 S K Mukherji *Clinical Applications of Magnetic Resonance Spectroscopy* New York John Willey & Sons (1998)

8 I R Young and H C Charles *MR Spectroscopy Clinical Applications and Techniques* Cambridge Martin Dunitz (1996)

9 P J Hore *J Magn Reson* **55** (1983) 283

10 P A Bottomley, W A Edelstein, T H Foster and W A Adams *Proc Natl Acad Sci USA* **82** (1985) 2148

11 C L Dumoulin *Magn Reson Med* **2** (1985) 583

12 A Haase, J Frahm, W Hanicke and D Matthei *Phys Med Biol* **30** (1985) 341

13 N Salibi and M A Brown *Clinical MR Spectroscopy: First Principles* New York John Wiley & Sons (1998)

14 P A Bottomley *Ann N Y Acad Sci* **508** (1987) 333

15 M Decorps and D Bourgeois *NMR : Basic Principles and Progress* **27** (1992) 119

16 J J H Ackerman, T H Grove, C G Wong, D G Gadian and G K Radda *Nature* **282** (1980) 167

17 D J Hoult *J Magn Reson* **33** (1979) 183

18 T A D Cadoux-Hudson, M J Blackledge and G K Radda *FASEB J* **3** (1989) 2660

19 T A D Cadoux-Hudson, B Rajagopalan, J G G Ledingham and G K Radda *Clin Sci* **79** (1990) 1

20 C T Moonen, S E Anderson and S Unger *Magn Res Med* **5** (1987) 296

21 T Nakada and I L Lee *Magn Reson Imaging* **7** (1989) 543

22 R E Gordon, P E Hanley, D Shaw, D G Gadian, G K Radda, P Stout, P J Bore and L Chan *Nature* **287** (1980) 736

23 P A Bottomley, T H Foster and R D Darrow *J Magn Reson* **59** (1984) 338

24 R J Orididge, A Connelly and J A B Lohman *J Magn Reson* **66** 1(986) 283

25 J Frahm, K D Merbolt and W Hanicke *J Magn Reson* **72** (1987) 502

26 J Frahm, H Bruhn, M L Gyngell, K D Merboldt, W Hanicke and R Sauter *Magn Reson Med* **9** (1989) 79

27 P A Bottomley *U S Patent 4* **480** (1984) 228

28 R J Orididge, M R Bendall, R E Gordon and A Connelly. *Magnetic Resonance in Biology and Medicine* (Eds. G Govil, C L Khetrapal, A Saran and A S Tata) McGraw Hill New Delhi (1985) 387

29 T R Brown, B M Kincaid and K Ugurbil *Proc Natl Sci USA* **79** (1982) 3523

30 A A Maudsley, S K Hilal, W H Perman, and H E Simon *J Magn Reson* **51** (1983) 147

31 P R Luyten, A J H Marien, W Heindel, P H J van Gerwen, K Herholz, J A den Hollander, G Friedmann and W D Heiss *Radiology* **176** (1990) 791

32 P A Bottomley, H C Charles, P B Roemer, D Falmig, H Engeseth, W A Edelstein and O M Mueller *Magn Reson Med* **7** (1988) 319

33 D B Twieg, D J Meyerhoff, B Hubesch, K Roth, B Sappey-Marinier, M D Boska, J R Gober, S Schaeffer and M W Weiner *Magn Reson Med* **12** (1989) 291

34 C M Segebarth, D F Baleriaux, P R Luyten and J A den Hollander *Magn Reson Med* **13** (1990) 62

35 R Sauter, M Schneider, R Wicklow and H Kolem *Electromedica* **60** (1992) 31

36 D J Hoult, S J W Busby, D G Gadian, G K Radda, R F Richards and P J Seeley *Nature* **252** (1974) 285

37 C M Segebarth D Baleriaux, D A Arnold, P R Luyten and J A den Hollander *Radiology* **165** (1987) 215

38 J Maris, A Evans, A Mclaughlin, G J D'Angio, L Bolinger, H Manos and B Chance *N Engl J Med* **312** (1985) 1500

39 S R Williams, H A Crockard and Gadian DG *Cerebrovasc Brain Metab Rev* **1** (1989) 91

40 F Podo *NMR Biomed* **12** (1999) 413

41 P L Hope, E B Cady, P S Tofts, D T Delpy, P S Tofts, A Chu, P A Hamilton, E O Reynolds and D R Wilke *Lancet* **2** (1984) 366

42 D P Younkin, M Delivoria-Papadopoulos, J C Leonard, V H Subramanian S Eleff, J S Leigh Jr and B Chance *Ann Neurol* **16** (1984) 581

43 D Boesch, R Gruetter, E Martin, G Duc and K Wuthrich *Radiology* **172** (1989) 197

44 S R Levine, J A Helpren, K M Welch, AM Vande Linde, K L Sawaya, E E Brown, N M Ramaden, R K Deveshwar and R J Orididge *Radiology* **185** (1992) 537

45 J E Jenson, D J Drost, R S Menon and P C Williamson *NMR Biomed* **15** (2002) 338

46 B Hubesch, D Sappey-Marinier, K Roth, D J Meyerhoff, G B Matson and M W Weiner *Radiology* **174** (1990) 401

47 CM Segebarth, DF Baleriaux, R de Beer, D van Ormondt, A Marien P R Luyten and J A den Hollander *Magn Reson Med* **11** (1989) 349

48. D Maintz, W Heindel, H Kugel, R Jaeger and K J Lackner *NMR Biomed* **15** (2002) 18

49 D L Arnold, E A Shoubridge, W Feindel and J G Villemure *J Neurol Sci* **14** (1987) 570

50 Z Argov, M Lofberg and D L Arnold *Muscle Nerve* **23** (2000) 1316

51 D J Taylor *Semin Musculoskel Radiol* **4** (2000) 481

52 A Heerschap, C Houtman, H J in 't Zandt, A J van den Bergh and B Wieringa *Proc Nutr Soc* **58** (1999) 861

53 R G Miller, D Giannini, H S Milner-Brown, R B Layzer, A P Koretsky, D Hooper and M W Weiner *Muscle Nerve* **10** (1987) 810

54 J Maurer, P Konstanczak, O Sollner, T Ehrenstein, F Knollmann, R Wolff, T J Vogl and R Felix *Acta Radiol* **40** (1999) 73

55 T Kutsuzawa, S Shioya, D Kurita, M Haida and H Yamabayashi *Med Sci Sports Exer* **33** (2001) 901

56 R K Gupta, R D Mittal, K N Aggarwal and D K Agarwal *Acta Paediat* **83** (1994) 327

57 A Thompson, A Damyanovich, A Madapallimattam, D Mikalus, J Allord and K N Jeejeebhoy *Am J Clin Nutr* **67** (1998) 39

58 B D Ross, G K Radda, D G Gadian, G Rocker, M Esiri and J Falconer-Smith *N Engl J Med* **304** (1981) 1338

59 G Vita, A Toscano, N Bresolin, G Melola, F Fortunato, A Baradello, B Barbiroli, C Frassineti, P Zaniol and C Messina J *Neurol* **241** (1994) 289

60 G J Kemp, D J Taylor, J F Dunn, S P Frostick and G K Radda *J Neurol Sci* **116** (1993) 201

61 D P Youkin, P Berman, J Sladky, C Chee, W Bank and B Chance *Neurology* **37** (1987) 165

62 B Barbiroli, R Funicello, S Iotti, P Montagna, A Ferlini and P Zaniol *J Neurol Sci* **109** (1992) 188

63 R Lodi, G J Kemp, F Muntoni, G H Thompson, C Rae, J Taylor, P Styles and D J Taylor *Brain* **122** (1999) 121

64 B Barbiroli, R Funicello, A Ferlini, P Montagna and P Zaniol *Muscle Nerve* **15** (1992) 344

65 S Felber, D Skaldal, M Wyss, C Kremser, A Koller and W Sperl *Neurol Res* **22** (2000) 145

66 J H Park, J P Vansant, N G Kumar, S J Gibbs, M S Curvin, R R Price, C L Partain and A E James *Radiology* **177** (1990) 473

67 J H Park, S Kari, L E King Jr and N J Olsen *NMR Biomed* **1** (1998) 245

68 G Cea, D Bendahan, D Manners, D H Jones, R Lodi, P Styles and D J Taylor *Brain* **125** (2002) 1635

69 S M Ronen and M O Leach *Breast Cancer Res* **3** (2001) 36

70 M O Leach, M varnil, J Glaholm, J A D Smith, D J Collins, G S Payne, J C Sharp, S M Ronen, V R McCready, T J Powles and I E Smith *NMR Biomed* **11** (1998) 314

71 C J Twelves, D A Porter, M Lowry, N A Dobbs, PE Graves, M A Smith, R D Rubens and M A Richards *Br J Cancer* **69** (1994) 1151

72 G S Payne, M Dowsett and M O Leach *Breast* **3** (1994) 20

73 P E Sijens, H K Wijrdeman, M A Moerland, C J Bakker, J W Vermeulen and P R Luyten *Radiology* **169** (1988) 615

74 J Glaholm, M O Leach, D J Collins, J Mansil, J C Sharp, A Madden, I E Smith and V R Mc Cready *Lancet* **1** (1989) 1326

75 J M Park and J H Park *Korean J Radiol* **2** (2001) 80

76 H Degani, R Horowitz and Y Itzchak *Radiology* **161**(1986) 53

77 T C Ng, S Graundfest, S Vijaykumar, N J Baldwin, A W Majors, I Karalis, T F Meaney, K H Shin, F J Thomas and R Tubbs *Magn Reson Med* **10** (1989) 125

78 M L Simmons, C G Frondoza and J T Coyle *Neuroscience* **45** (1991) 37

79 M C Fleming and O H Lowry *J Neurochem* **13** (1966) 779

80 J V Nadler and J R Cooper *J Neurochem* **19** (1972) 313

81 B L Miller *NMR Biomed* **4** (1991) 47

82 H Kugel, W Heindel, R I Ernestus, J Bunke, R du Mesnil and G Friedmann *Radiology* **183** (1992) 701

83 R Kries, T Ernst and B D Ross *Magn Reson Med* **30** (1993) 424

84 M Terpstra, K Ugurbil and R Gruetter *Magn Reson Med* **47** (2002) 1009

85 J Shen, D L Rothman and P Brown *Magn Reson Med* **47** (2002) 447

86 B D Ross and T Michaelis *Mag Res Q* **10** (1994) 191

87 M J Fulham, A Bizzi, M J Dietz, H H Shih, R Raman, G S Sobering, J A Frank, A J Dwyer, J R Alger and G Chiro *Radiology* **185** (1992) 675

88 R Kreis, T Ernst and B D Ross *Science* **216** (1982) 1325

89 J A Sanders Magnetic Resonance Spectroscopy *Functional Imaging* (Eds. W W Orrison, J D Lewine, J A Sanders *et al.*) St Louis Mosby (1995) 419

90 S R Williams, D G Gadian and E A Proctor *J Magn Reson* **66** (1986) 562

91 A Knuttel and R Kimmich *Magn Reson Med* **10** (1989) 404

92 H P Hetherington, M J Avison and R G Shulman *Proc Natl Acad Sci USA* **82** (1985) 3115

93 A J Cooper and F Plum *Physiol Rev* **67** (1987) 440

94 B D Ross NMR *Biomed* **4** (1991) 59

95 R S Badar-Goffer, O Ben-Yoseph, H S Bachelard, and P G Morris *Biochem J* **282** (1992) 225

96 S Ceodan, R Parrilla and J Santoro *FEBS Lett* **187** (1985) 167

97 B L Miller, R A Moats, T Shonk, T Ernst, Woolley S and B D Ross *Radiology* **187** (1993) 433

98 R Kreis and BD Ross *Radiology* **184** (1992) 123

99 R Kreis, N A Farrow and B D Ross *NMR Biomed* **4** (1991) 109

100 I Tkac, P Anderson, G Andriany, H Merkle, K Ugurbil and R Gruetter *Magn Reson Med* **46** (2001) 451

101 T Michaelis, K D Merbolt, H Bruhn, W Hanicke and J Frahm *Radiology* **187** (1993) 219

102 M Castillo, L Kwock and S K Mukherji *AJNR Am J Neuroradiol* **17** (1996) 1

103 X Leclerc, T A Huisman and A G Sorensen *Curr Opin Oncol* **14** (2002) 292

104 I M Burlscher and S Holtas *J Magn Reson Imaging* **13** (2001) 560

105 R Jayasundar and P Raghunathan *Magn Reson Imaging* **15** (1997) 223

106 R Jayasundar *Neurol (India)* **50** (2002) 267

107 H Bruhn, J Frahm, M L Gyngell, K D Merboldt, W Hanicke R Sauter and C Hamburger *Radiology* **172** (1989) 541

108 R N Sener *Comput Med Imaging Graph* **26** (2002) 187

109 P E Sijens, M V Knopp, A Brunetti, K Wicklow, B Alfano, P Bachert, J A Sanders, A E Stillman, H Katt and R Sauter *Magn Reson Med* **33** (1995) 818

110 M Hartmann W S Herminghaus, T Krings, G Marquardt, H Lanfermann, U Pilatus and F E Zanella *Neuroradiol* **44** (2002) 371

111 H Ishimaru, M Morikawa, S Iwanaga, M Kaminogo, M Ochi and K Hayashi *Eur J Radiol* **11** (2001) 1784

112 M Law, S Cha, E A Knopp, G Jonson, J Arnett and A W Litt *Radiology* **222** (2002) 715

113 S Herminghaus, U Pilatus, W Moller-Hartmann, P Raab, H Lanfermann, W Scholte and F E Zanella *NMR Biomed* **15** (2002) 385

114 A A Mellati, M Yucel, N Altinors and U Gunduz *Cancer Biochem Biophys* **13** (1992) 33

115 A Bizzi, B Movsas, G Tedeschi, C L Phillips, P Okunieff, J R Alger and G Di Chiro *Radiology* **194** (1995) 271

116 J R Gober *Neuroimaging Clin N Am* **3** (1993) 779

117 R Tarnaswki, M Sokol, P Pieniazek, B Maciejewski, J Walecki, L Miszczyk and T Krupska *Int J Radiat Oncol Biol Phys* **52** (2002) 1271

118 P B Barker, J H Gillard, P C M van Zijl, B J Soher, D F Hanley, A M Agildere, S M Oppenheimer and R N Bryan *Radiology* **192** (1994) 723

119 P E Ricci Jr *Neuroimaging Clin N Am* **8** (1998) 881

120 D E Saunders, F A Howe, A van den Boogart, M A McLean, J R Griffiths and M M Brown *Stroke* **26** (1995) 1007

121 G D Grahm, J H Hwang, D L Rothman and J W Prichard *Stroke* **32** (2001) 2797

122 R K Gupta, T F Cloughesy, U Sinha, J Garakian, J Lazareff, G Rubino, L Rubino, D P Becker, H V Vinters and J R Alger *J Neurooncol* **50** (2000) 215

123 C Remy, S Grand, ES Lai, V Belle, D Hoffmann F Berger, F Esteve, A Ziegler, J F Le Bas and A L Benabid *Magn Reson Med* **34** (1995) 508

124 S K Venkatesh, R K Gupta, L Pal, N Husain and M Husain *J Magn Reson Imaging* **14** (2001) 8

125 R Jayasundar, V P Singh, V Jain, P Raghunathan and A K Banerji *NMR Biomed* **12** (1999) 1

126 V J Vanda, J H Sherman and D S Luciano *Human Physiology* London McGraw Hill (1999)

127 R Jayasundar and V P Singh *Neurology (India)* **84** (2001) 1016

128 D L Rothman, K L Behar, J Prichard and O A Petroff 1997 *Magn Reson Med* **38** (1997) 924

129 J W Pan, J R Hamm, D L Rothman and R G Shulman *Proc Natl Acad Sci USA* **85** (1988) 7836

130 R Van Sluis, Z M Bhujwalla, N Raghunand, P Ballesteros, J Alvarez, S Cerdan, J P Galons and R J Gilles *Magn Reson Med* **41** (1999) 743

131 N R Jagannathan, N G Desai and P Raghunathan *Magn Reson Imaging* **14** (1996) 553

132 N R Jagannathan, N Tandon, P Raghunathan and N Kochupillai *Dev Brain Res* **109** (1998) 179

133 J A Stanley *Can J Psychiatry* **47** (2002) 315

134 K Kasai, A Iwanami, H Yamasue, N Kuroki, K Nakagome and M Fukuda *Neurosci Res* **43** (2002) 93

135 D P Auer, M Wilke, A Grabner, J O Heidenreich, T Bronisch and T C Wetter *Schizophr Res* **52** (2001) 87

136 G K Malik, M Pandey, R Kumar, S Chawla, B Rathi and R K Gupta *Eur J Radiol* **43** (2002) 6

137 B L Miller, R A Moats, T Shonk, T Ernst, S Wolley and B D Ross *Radiology* **187** (1993) 433

138 R A Moats, T Ernst, T K Shonk and B D Ross *Magn Reson Med* **32** (1994) 110

139 T Shonk and B D Ross *Magn Reson Med* **195** (1995) 65

140 J M Constants, D J Meyerhof, J Gerson, S MacKay, D Norman, G Fein and M W Weiner *Radiology* **197** (1995) 517

141 S MacKay, F Ezekiel, V Di Sclafani, D J Meyerhoff, J Gerson, D Norman, G Fein and M W Weiner *Radiology* **198** (1996) 537

142 S Mackay, D J Meyerhoff, J M Constans, D Norman, G Fein and M W Weiner *Arch Neurol* **53** (1996) 167

143 R Jayasundar, A K Sahani, S Gaikwad, S Singh and M Behari *Magn Reson Imaging* **20** (2002) 131

144 F Cendes, F Andermann, M C Preul and D L Arnold *Ann Neurol* **35** (1994) 211

145 D G Gadian, A Connelly, J S Duncan, J H Cross, F L Kirknam, C L Johnson, F Vargha-Khadem, B G Nevile and G D Jackson *Acta Neurol Scand* **152** (1994) 116

146 J W Hugg, K D Laxer, G B Matson, A A Maudsley and M W Weiner *Ann Neurol* **34** (1993) 788

147 J Constantinidis, J A Malko, S B Peterman, R C J Long, C M Epstein, D Boor, J C Hoffman, L Shutter and J D Weissman *Br J Radiol* **69** (1996) 15

148 A Connelly, G D Jackson, J S Duncan, M D King and D G Gadian *Neurology* **44** (1994) 1411

149 P M Matthews, F Andermann and D L Arnold *Neurology* **40** (1990) 985

150 J S Duncan *Epilepsia* **37** (1996) 598

151 D L Rothman, O A Petroff, K L Behar and R H Mattson *Proc Natl Acad Sci USA* **90** (1993) 5662

152 P B Barker, R R Lee and J C Mc Arthur *Radiology* **195** (1995) 58

153 M Castillo, L Kwock and SK Mukherji *AJNR Am J Neuroradiol* **17** (1996) 1

154 P A Narayana, J D Hazle, E F Jackson, L K Fotedar and M V Kulkarni *Magn Reson Imaging* **6** (1998) 481

155 H Bruhn, J Frahm, M L Gyngell, K D Merboldt, W Hanicke and R Sauter *Magn Reson Med* **17** (1991) 82

156 F Schick, B Eismann, W I Jung, H Bungers, M Bunse and O Lutz *Magn Reson Med* **29** (1993) 158

157 L Jouvensal, P G Carlier and G Bloch *Magn Reson Med* **36** (1996) 487

158 C Boesch and R Kreis *Ann N Y Acad Sci* **904** (2000) 25

159 N R Jagannathan and S Wadhwa *Magn Reson Imaging* **20** (2002) 113

160 N R Jagannathan, M Singh, V Govindaraju, P Raghunathan, O Coshic, P K Julka and G K Rath *NMR Biomed* **11** (1998) 414

161 N R Jagannathan, M Kumar, P Raghunathan, O Coshic, P K Julka and G K Rath *Curr Sci* **76** (1999) 777

162 C J G Bakker and J Vriend *Phys Med Biol* **33** (1983) 331

163 W B Mackinnon, L Huschtscha, K Dent, R Hancock, C Paraskeva C and C E Mountford *Int J Cancer* **59** (1994) 248

164 N R Jagannathan, M Kumar, V Seenu, O Coshic, S N Dwivedi, P K Julka, A Srivastava and G K Rath *Br J Cancer* **84** (2001) 1016

165 D K W Yeung, H S Cheung and G M K Tse *Radiology* **220** (2001) 40

166 K A Kvistad, I J Bakken, I S Gribbested, R J B Ehrnholm, L Steiner, H E Fjosne and O. Haraldseth *J Magn Reson Imaging* **10** (1999) 159

167 J R Roebuck, K M Cecil, M D Schnall and R E Lenkinski *Radiology* **209** (1998) 269

168 W B Mackinnon, P A Barry, P L Malycha, D J Gillett, P Russel, C L Lean, S T Doran, B H Barra Clough, M Bilous and C E Mountford *Radiology* **204** (1997) 661

169 R Katz-Brull, R Margalit, P Bendel and H Degani *MAGMA* **6** (1998) 44

170 R Katz-Brull, D Seger, D Rivenson-Segal, E Ruskin and H Degani *Cancer Res* **62** (2002) 1966

171 G I Shulman, G Cline, W C Schumann, V Chandramouli, K Kumaran and B R Landau *Am J Physiol* **259** (1990) 335.

172 M Roden and G I Shulman *Annu Rev Med* **50** (1999) 277

173 R A Komoroski, J E O Newton, D Cardwell, J Sprigg, J Pearce and C N Karson *Magn Reson Med* **31** (1994) 204

174 A N Stevens, P G Morris, R A Iies, P W Sheldon and J R Griffiths *Br J Cancer* **50** (1984) 113

175 P J Sijens, Y Huang, N J Baldwin and T C Ng *Cancer Res* **51** (1999) 1384

176 P Mohanakrishnan, L Hutchins, S Nauke, J Sprigg, D Cardwell M R Williamson , R A Komoroski and N R Jagannathan *Curr Sci* **76** (1999) 677

177 W Wolf, M J Albright, M S Silver, H Weber, V Reichardt and R Sauer *Magn Reson Imaging* **5** (1987) 165

178 W Wolf, C A Presant, K L Servis, A El-Tahtawy, M J Albright, P B Barker, I I I Ring, R Atkinson, D Ong, R King, M Singh, M Ray, M Wiseman, C Blayney, and D J Shani *Proc Natl Acad Sci USA* **87** (1990) 492

179 P F Renshaw, A R Guimaraes, M Fava, J F Rosenbaus, J D Pearlman, J G Flood, P R Puopolo, K Clancy and R G Gonzalez *Am J Psychiatry* **149** (1992) 1592

180 R G Gonzalez, A R Guimaraes, G S Sachs, J F Rosenbaum, M Garwood and P F Renshaw *Am J Neuroradiol* **14** (1993) 1027

181 R A Komoroski, J E O Newton, E Walker, D Cardwell, N R Jagannathan, S Ramaprasad and J Sprigg *Magn Reson Med* **15** (1990) 347

182 P A Narayana, M V Kulkarni and S D Mehta NMR of ^{23}Na in biological systems *Magnetic Resonance Imaging* (Eds. *C L Partain, R R Price and J Patton)* Philadelphia Saunders (1988)

183 M Horn, C Weidensteiner, H Scheffer, K Prezyklenk, M von Kienlin and S Neubauer *MAGMA* **11** (2001) 42

184 M Horn, C Weidensteiner, H Scheffer, M Meininger, M de Groot, H Remkes, C Dienesch, K Prezyklenk, M von Kienlin and S Neubauer *Magn Reson Med* **45** (2001) 756

185 W R Adam, A P Koretsky and M W Weiner *Biophys J* **51** (1986) 265

186 W R Adam, A P Koretsky and M W Weiner *Am J Physiol* **254** (1988) F 401

187 N B Redford, E E Babcock, A Richmann, L Szczepaniak, C R Mallory and A D Sherry *Magn Reson Med* **40** (1998) 544